(12) INTERNATIONAL APPLICATION PUBLISHED UNDER THE PATENT COOPERATION TREATY (PCT)

(19) World Intellectual Property Organization
International Bureau

(43) International Publication Date
17 July 2003 (17.07.2003)

PCT

(10) International Publication Number
WO 03/058904 A1

(51) International Patent Classification[7]: H04L 27/00

(21) International Application Number: PCT/US02/37532

(22) International Filing Date:
21 November 2002 (21.11.2002)

(25) Filing Language: English

(26) Publication Language: English

(30) Priority Data:
60/344,012 27 December 2001 (27.12.2001) US
10/141,628 6 May 2002 (06.05.2002) US

(71) Applicant: **BERMAI, INC.** [US/US]; 410 Cambridge Avenue, 2nd floor, Palo Alto, CA 94306 (US).

(72) Inventors: **KIM, Younggyun**; 303 Huntington Street, Irvine, CA 92620 (US). **RAD, Farshid, R.**; 700 10th Avenue SE, Apt. 17, Minneapolis, MN 55414 (US). **BRICKNER, Barrett, J.**; 9206 Heatherton Ridge Drive, Savage, MN 55378 (US). **MOON, Jaekyun**; 3450 Merrimac Lane North, Plymouth, MN 55447 (US).

(74) Agent: **SHUMAKER, Steven, J.**; Shumaker & Sieffert, P.A., 8425 Seasons Parkway, Suite 105, St. Paul, MN 55125 (US).

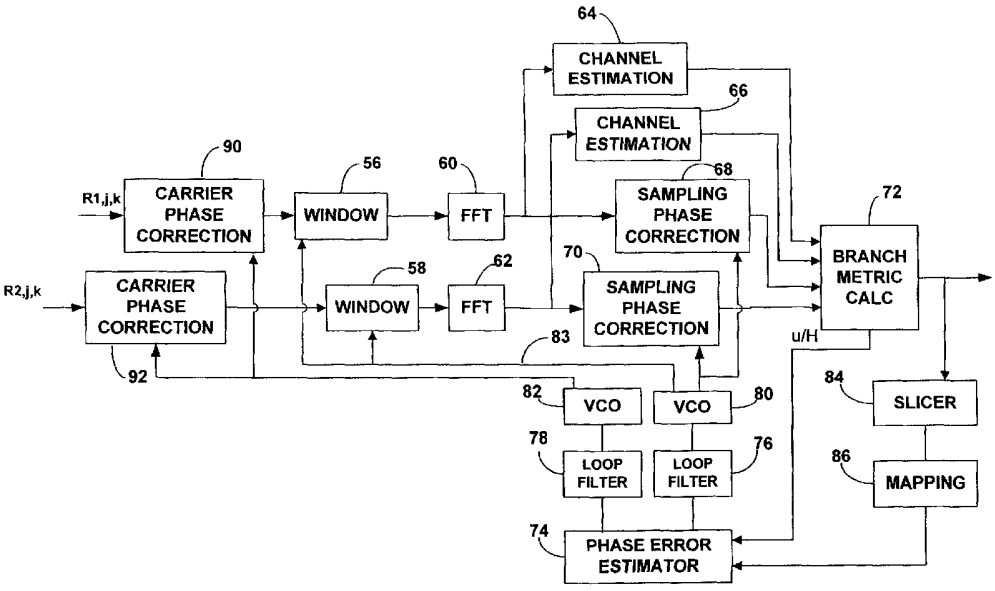
(81) Designated States *(national)*: AE, AG, AL, AM, AT, AU, AZ, BA, BB, BG, BR, BY, BZ, CA, CH, CN, CO, CR, CU, CZ, DE, DK, DM, DZ, EC, EE, ES, FI, GB, GD, GE, GH, GM, HR, HU, ID, IL, IN, IS, JP, KE, KG, KP, KR, KZ, LC, LK, LR, LS, LT, LU, LV, MA, MD, MG, MK, MN, MW, MX, MZ, NO, NZ, OM, PH, PL, PT, RO, RU, SD, SE, SG, SI, SK, SL, TJ, TM, TN, TR, TT, TZ, UA, UG, UZ, VN, YU, ZA, ZM, ZW.

(84) Designated States *(regional)*: ARIPO patent (GH, GM, KE, LS, MW, MZ, SD, SL, SZ, TZ, UG, ZM, ZW), Eurasian patent (AM, AZ, BY, KG, KZ, MD, RU, TJ, TM), European patent (AT, BE, BG, CH, CY, CZ, DE, DK, EE, ES, FI, FR, GB, GR, IE, IT, LU, MC, NL, PT, SE, SK, TR), OAPI patent (BF, BJ, CF, CG, CI, CM, GA, GN, GQ, GW, ML, MR, NE, SN, TD, TG).

Published:
— *with international search report*

[Continued on next page]

(54) Title: JOINT EQUALIZATION, SOFT-DEMAPPING AND PHASE ERROR CORRECTION IN WIRELESS SYSTEM WITH RECEIVE DIVERSITY



(57) Abstract: A wireless communication technique enables equalization, soft mapping (86) and phase error estimation (74) functions to be performed jointly based on multiple observations of a transmitted symbol in wireless communication systems employing receive diversity. Multiple observations of a symbol are obtained from multiple antenna paths in a wireless receiver. Equalization, soft demapping (86), and phase error estimation (74) functions can be integrated within shared hardware, rather than distributed among separate hardware blocks, promoting reduced size, complexity and cost in a wireless receiver.

WO 03/058904 A1

For two-letter codes and other abbreviations, refer to the "Guidance Notes on Codes and Abbreviations" appearing at the beginning of each regular issue of the PCT Gazette.

JOINT EQUALIZATION, SOFT-DEMAPPING AND PHASE ERROR CORRECTION IN WIRELESS SYSTEM WITH RECEIVE DIVERSITY

FIELD

[0001] The invention relates to wireless communication and, more particularly, to techniques for demodulation of wireless signals transmitted in a wireless communication system.

BACKGROUND

[0002] Wireless communication involves transmission of encoded information on a modulated radio frequency (RF) carrier signal. A wireless receiver includes an RF antenna that receives a wireless signal, and a demodulator that converts the RF signal to a baseband. In a multi-carrier wireless communication system, such as an orthogonal frequency division multiplexing (OFDM) system, transmitted signals are susceptible to multi-path scattering and reflection, which can cause interference between information transmitted on different symbols. For this reason, the receiver typically includes a channel estimator that measures fluctuation of the channel response. The receiver uses the measured channel response to adjust the incoming signals, and compensate for channel effects that could cause interference.

[0003] The receiver demodulates the communication signal using an oscillator that operates independently of the transmitter carrier frequency. The receiver periodically samples the received analog carrier signal, and extracts a communication signal using digital signal processing techniques. Differences between the carrier frequency and the demodulation frequency of the receiver may contribute phase rotation to the frequency domain signal. This frequency error produces a phase shift that increases as time progresses, and can be accompanied by additive phase noise. Accordingly, the receiver also may perform phase error estimation and correction to improve decoding accuracy.

[0004] Encoding techniques such as quadrature amplitude modulation (QAM) involve mapping of a finite number of bits to each transmitted symbol to encode information in the wireless signal. To decode the information, the receiver demaps the symbols, typically using a soft demapping algorithm. A soft decision for a given bit can be

obtained using a log likelihood ratio. The soft decisions are used to calculate branch metrics for a convolutional decoder such as a Viterbi decoder.

[0005] Equalization, soft demapping and phase error estimation represent some of the features that contribute to the size, complexity and cost of a wireless receiver. Such features ordinarily are necessary in a wireless communication system, however, to ensure effective communication of desired information.

SUMMARY

[0006] The invention is directed to wireless communication techniques that enable equalization, soft demapping and phase error estimation functions to be performed jointly based on multiple observations of a transmitted symbol in wireless communication systems employing receive diversity. Multiple observations of a transmitted symbol are obtained from multiple antenna paths in a wireless receiver. The invention enables the equalization, soft demapping and phase error estimation functions to be integrated within shared hardware, rather than distributed among separate hardware blocks. In this manner, the invention can reduce the size, complexity and cost of a wireless receiver.

[0007] The invention may be applied, for example, to a multi-carrier (MC) wireless communication system, such as an OFDM system. In an OFDM system, a number of QAM symbols are transmitted in parallel in the time-domain via inverse Fourier transformation. The invention may enable equalization, soft demapping and phase error estimation functions to be performed jointly for multiple observations of a transmitted symbol transmitted in an OFDM wireless communication system employing receive diversity. The multiple observations of a transmitted symbol are the outputs of Fourier transformers that are applied to the multiple antenna paths in the OFDM wireless receiver. In the OFDM example, symbol observations can be obtained from fast Fourier transform (FFT) outputs.

[0008] In one embodiment, the invention provides a method comprising receiving wireless signals via one or more antennas, demodulating the wireless signals to produce observations of a transmitted symbol, weighting each of the observations with a complex conjugate of an estimated channel response for the corresponding antenna, combining the weighted observations to form a combined observation, and generating one or more soft decision bits indicative of the transmitted symbol for the

combined observation according to soft demapping rules based on a subset of the transmitted symbol constellation.

[0009] In another embodiment, the invention provides a method comprising receiving wireless signals via one or more antennas, demodulating the wireless signals to produce observations of a transmitted symbol, weighting each of the observations with a complex conjugate of an estimated channel response for the corresponding antenna, combining the weighted observations to form a combined observation, generating one or more soft decision bits indicative of the transmitted symbol for the combined observation according to soft demapping rules based on a subset of the transmitted symbol constellation, and estimating the phase error using the soft decision bits.

[0010] In another embodiment, the invention provides a wireless receiver comprising one or more antennas that receive wireless signals, a demodulator that demodulates the wireless signals to produce observations of a transmitted symbol, an equalizer that weights each of the observations with a complex conjugate of an estimated channel response for the corresponding antenna, a soft demapper unit that combines the weighted observations to form a combined observation, and generates one or more soft decision bits indicative of the transmitted symbol for the combined observation according to soft demapping rules based on a subset of the transmitted symbol constellation.

[0011] In another embodiment, the invention provides a wireless receiver comprising one or more antennas that receive wireless signals, a demodulator that demodulates the wireless signals to produce observations of a transmitted symbol, an equalizer that weights each of the observations with a complex conjugate of an estimated channel response for the corresponding antenna, a soft demapper unit that combines the weighted observations to form a combined observation, and generates one or more soft decision bits indicative of the transmitted symbol for the combined observation according to soft demapping rules based on a subset of the transmitted symbol constellation, and an estimator the phase error using the soft decision bits.

[0012] In a further embodiment, the invention provides a method comprising receiving orthogonal frequency division multiplexing (OFDM) wireless signals via multiple antennas, demodulating the wireless signals to produce observations of a quadrature amplitude modulation (QAM) symbol, combining the observations to form a combined observation, and generating one or more soft decision bits indicative of

the QAM symbol for the combined observation according to piecewise linear soft demapping rules.

[0013] In another embodiment, the invention provides a method comprising receiving orthogonal frequency division multiplexing (OFDM) wireless signals via multiple antennas, demodulating the wireless signals to produce observations of a quadrature amplitude modulation (QAM) symbol, combining the observations to form a combined observation, and generating one or more soft decision bits indicative of the QAM symbol for the combined observation according to piecewise linear soft demapping rules, and estimating the phase error using the soft decision bits.

[0014] In an added embodiment, the invention provides a receiver comprising multiple antennas that receive orthogonal frequency division multiplexing (OFDM) wireless signals via multiple antennas, a demodulator that demodulates the wireless signals to produce observations of a quadrature amplitude modulation (QAM) symbol, a soft demapper unit that combines the observations to form a combined observation, and generates one or more soft decision bits indicative of the QAM symbol for the combined observation according to piecewise linear soft demapping rules.

[0015] In an added embodiment, the invention provides a receiver comprising multiple antennas that receive orthogonal frequency division multiplexing (OFDM) wireless signals via multiple antennas, a demodulator that demodulates the wireless signals to produce observations of a quadrature amplitude modulation (QAM) symbol, a soft demapper unit that combines the observations to form a combined observation, and generates one or more soft decision bits indicative of the QAM symbol for the combined observation according to piecewise linear soft demapping rules, and an estimator that estimates the phase error using the soft decision bits.

[0016] In another embodiment, the invention provides a method comprising applying a soft decision function to generate soft decision bits for a combined transmitted symbol observation produced from wireless signals received via multiple receive paths, wherein the soft decision function defines soft demapping rules based on a subset of the transmitted symbol constellation.

[0017] In a further embodiment, the invention provides a receiver comprising a soft demapper unit that applies a soft decision function to generate soft decision bits for a combined QAM symbol produced from wireless signals received via multiple receive

paths, wherein the soft decision function defines soft demapping rules based on a subset of the transmitted symbol constellation.

[0018] The invention may provide one or more advantages. The equalization, soft demapping and phase error estimation functions can be performed jointly within shared hardware. Accordingly, the invention promotes reduced size, complexity and cost of hardware components in a multi-carrier wireless receiver such as an OFDM wireless receiver. In addition, the invention promotes increased efficiency and accuracy in the demodulation of transmitted symbols in a wireless communication system. For example, the use of multiple receive paths permits increased signal-to-noise ratio in the detection of the transmitted symbol.

BRIEF DESCRIPTION OF THE DRAWINGS

[0019] FIG. 1 is a block diagram illustrating a wireless communication network.

[0020] FIG. 2 is a block diagram illustrating a wireless communication device useful in the network of FIG. 1.

[0021] FIG. 3 is a block diagram illustrating a constellation of binary phase shift keying (BPSK) symbols.

[0022] FIG. 4 is a block diagram illustrating a constellation of 4-QAM symbols.

[0023] FIG. 5 is a block diagram illustrating a constellation of 16-QAM symbols.

[0024] FIG. 6 is a block diagram illustrating a constellation of 64-QAM symbols.

[0025] FIG. 7 is a graph illustrating piecewise soft decisions $\Lambda(b_1)$ and $\Lambda(b_2)$ summed over diversity paths for 16-QAM encoding.

[0026] FIG. 8 is a graph illustrating piecewise soft decisions $\Lambda(b_1)$, $\Lambda(b_2)$ and $\Lambda(b_3)$ summed over diversity paths for 64-QAM encoding.

[0027] FIG. 9 is a block diagram illustrating an exemplary soft demapping unit for BPSK decoding.

[0028] FIG. 10 is a block diagram illustrating an exemplary soft demapping unit for 4-QAM decoding.

[0029] FIG. 11 is a block diagram illustrating a soft demapping unit for 16-QAM decoding.

[0030] FIG. 12 is a block diagram illustrating a soft demapping unit for 64-QAM decoding.

[0031] FIG. 13 is a block diagram illustrating a soft demapping unit for 256-QAM decoding.

[0032] FIG. 14 is a block diagram illustrating a soft demapping unit for 1024-QAM decoding.

[0033] FIG. 15 is a block diagram illustrating a phase locked loop with frequency domain correction.

[0034] FIG. 16 is a block diagram illustrating an alternative phase locked loop with time and frequency domain correction.

[0035] FIG. 17 is a block diagram illustrating implementation of an exemplary phase error estimator for use in a phase locked loop as shown in FIG. 15 or FIG. 16.

[0036] FIG. 18 is a block diagram illustrating implementation of an alternative phase error estimator for use in a phase locked loop as shown in FIG. 15 or FIG. 16.

[0037] FIG. 19 is a block diagram illustrating implementation of another alternative phase error estimator for use in a phase locked loop as shown in FIG. 15 or FIG. 16.

[0038] FIG. 20 is a block diagram illustrating implementation of a further alternative phase error estimator for use in a phase locked loop as shown in FIG. 15 or FIG. 16.

[0039] FIG. 21 is a flow diagram illustrating joint performance of equalization, soft-demapping and phase error estimation functions.

DETAILED DESCRIPTION

[0040] FIG. 1 is a block diagram illustrating a wireless communication network 10. Wireless communication network 10 may be configured for joint performance of equalization, soft demapping and phase error estimation functions. In particular, the equalization, soft demapping and phase error estimation functions may be applied to multiple observations of a transmitted symbol received via a receive diversity antenna arrangement. The transmitted symbol may be, for example, a QAM symbol. Wireless communication network 10 may be a multi-carrier wireless network such as, for example, an OFDM wireless network.

[0041] As shown in FIG. 1, wireless communication network 10 may include one or more wireless access points 12 coupled to a wired network 14, e.g., via an Ethernet connection. Wireless access point 12 permits wireless communication between wired network 14 and one or more wireless communication devices 16A-16N (hereinafter 16). Each wireless communication device 16, as well as wireless access point 12,

may include two or more antennas that provide multiple receive paths for receive diversity, as will be described in further detail herein. Wireless access point 12 may integrate a hub, switch or router to serve multiple wireless communication devices 16. Wireless communication network 10 may be used to communicate data, voice, video and the like between devices 16 and network 14 according to a variety of different wireless transmission standards based on a multi-carrier communication technique such as OFDM.

[0042] FIG. 2 is a block diagram illustrating a wireless communication device 16 in further detail. As shown in FIG. 2, wireless communication device 16 may include at least two RF antennas 18A, 18B (hereinafter 18), a radio 20, modem 22, and media access controller 24 coupled to a host processor 26. Radio 20 and modem 22 function together as a wireless receiver. Wireless communication device 16 may take the form of a variety of wireless equipment, such as computers, personal computer cards, e.g., PCI or PCMCIA cards, personal digital assistants (PDAs), network audio or video appliances, and the like.

[0043] RF antennas 18 receive RF signals over one or more receive paths. In one embodiment, RF antennas 18 receive RF signals over multiple receive paths. Antenna 18A provides a first receive path 18A, and antenna 18B provides a second receive path. More than two antennas 18 may be provided in some embodiments for enhanced receive diversity. One of antennas 18, or a different antenna 19, may be used for transmission of RF signals within network 10. Radio 20 may include circuitry for upconverting transmitted signals to RF, and downconverting RF signals to baseband. In this sense, radio 20 may integrate both transmit and receive circuitry within a single transceiver component. In some cases, however, transmit and receive circuitry may be formed by separate transmitter and receiver components. For purposes of illustration, discussion herein will be generally limited to the receiver and demodulation aspects of radio 20 and modem 22.

[0044] Modem 22 encodes information in a baseband signal for upconversion to the RF band by radio 20 and transmission via a transmit antenna. Similarly, and more pertinent to the invention, modem 22 decodes information from RF signals received via antennas 18 and downconverted to baseband by radio 20. As will be described, the RF signals received by multiple antennas 18A, 18B may be demodulated to produce observations of QAM symbols. The observations are combined to form a combined observation for processing by a soft demapping unit within modem 22 to

produce the QAM symbol. Media access controller 24 interacts with host processor 26 to facilitate communication between modem 22 and a host wireless communication device 16, e.g., a computer, PDA or the like. Hence, host processor 26 may be a CPU within a computer or some other device. Radio 20, modem 22 and media access controller 24 may be integrated on a common integrated circuit chip, or realized by discrete components.

[0045] Wireless communication network 10 (FIG. 1) and wireless communication device 16 (FIG. 2) may conform to a wireless networking standard, such as the IEEE 802.11a standard. The IEEE 802.11a standard specifies a format for the radio frequency (RF) transmission of orthogonal frequency division multiplexed (OFDM) data. The OFDM symbols transmitted according to the IEEE 802.11a standard occupy a 20 MHz bandwidth, which is divided into 64 equally spaced frequency bands. Incorporation of multiple antennas 18 for receive diversity in an OFDM system, in accordance with the invention, can enhance the accuracy of signal demodulation and decoding. In addition, joint performance of equalization, soft demapping and phase error estimation for a observations obtained from multiple antenna receive paths may permit use of shared hardware, resulting in a wireless receiver having reduced cost, complexity and size.

[0046] Consider an OFDM wireless communication device 16, as shown in FIG. 2, with a single transmit antenna 19 and multiple receive antennas 18A, 18B, in accordance with the invention. In this example, every sub-carrier in each OFDM symbol received by wireless communication device 16 is modulated by a QAM symbol. Focusing on a particular OFDM symbol and a specific sub-carrier associated with the OFDM symbol, let r_i be the corresponding demodulated observation sample, i.e., an equalized FFT output, associated with the *i*th receive antenna, assuming two or more receive antennas 18 for receive diversity.

[0047] Also, let a_j denote the *j*th symbol in the applicable QAM constellation. A finite number of bits, e.g., $b_1 b_2 \cdots b_M$, are mapped to each QAM symbol. The soft decision associated with b_l, $1 \le l \le M$, can be obtained from the log likelihood ratio:

$$LLR(b_l) = \ln \frac{P(b_l = 1/\mathbf{R})}{P(b_l = 0/\mathbf{R})} = \ln \frac{\sum_{a_i \in A(b_l=1)} P(a_i/\mathbf{R})}{\sum_{a_j \in A(b_l=0)} P(a_j/\mathbf{R})} \quad (1)$$

where $\mathbf{R} = [r_1\ r_2 \cdots r_L]'$ is the vector of observation samples corresponding to L multiple receive antennas and the summation in the numerator or denominator, as applicable, is taken over all QAM symbols that share the common bit $b_l = 1$ ($b_l = 0$). It is now shown that a reduced-complexity soft decision detector can be obtained by using only a subset of the symbol constellation in (1). As an example, assuming that the symbols are equally likely, the log likelihood can be rewritten as:

$$LLR(b_l) = \ln \frac{\sum_{a_i \in A(b_l=1)} p(\mathbf{R}/a_i)}{\sum_{a_j \in A(b_l=0)} p(\mathbf{R}/a_j)} \approx \ln \frac{p(\mathbf{R}/a_{\min 1})}{p(\mathbf{R}/a_{\min 0})} \quad (2)$$

where

$$a_{\min 1} = \arg\max_{a_i \in A(b_l=1)} p(\mathbf{R} \mid a_i) \quad (3)$$

and

$$a_{\min 0} = \arg\max_{a_i \in A(b_l=0)} p(\mathbf{R} \mid a_i)\ . \quad (4)$$

Assuming additive Gaussian noise, the expression can be rewritten as:

$$LLR(b_l) \approx -\frac{1}{2}\mathbf{R}_1'\mathbf{C}^{-1}\mathbf{R}_1 + \frac{1}{2}\mathbf{R}_0'\mathbf{C}^{-1}\mathbf{R}_0 \quad (5)$$

where

$$\mathbf{R}_1 = \begin{bmatrix} r_1 - a_{\min 1} \\ r_2 - a_{\min 1} \\ \vdots \\ r_L - a_{\min 1} \end{bmatrix},\ \mathbf{R}_0 = \begin{bmatrix} r_1 - a_{\min 0} \\ r_2 - a_{\min 0} \\ \vdots \\ r_L - a_{\min 0} \end{bmatrix} \text{ and } \mathbf{C} = \begin{bmatrix} \sigma_1^2 & 0 & \cdots & 0 \\ 0 & \sigma_2^2 & \cdots & 0 \\ \vdots & \vdots & \ddots & \vdots \\ 0 & 0 & \cdots & \sigma_L^2 \end{bmatrix}.$$

The noise covariance matrix **C** is diagonal as the observations are assumed to be statistically independent. The variance σ_i^2 is the noise variance associated with the observation r_i. The expression (5) can be rewritten as:

$$LLR(b_l) \approx -\frac{1}{2}\sum_{i=1}^{L}\frac{1}{\sigma_i^2}\left|r_i - a_{\min 1}\right|^2 + \frac{1}{2}\sum_{i=1}^{L}\frac{1}{\sigma_i^2}\left|r_i - a_{\min 0}\right|^2 . \qquad (6)$$

Letting u_i and H_i denote the unequalized FFT output sample and the channel response associated with the ith antenna, respectively, expression (6) can be rewritten as:

$$\begin{aligned} 2\sigma_n^2 \cdot LLR(b_l) &\approx -\sum_{i=1}^{L}\left|H_i\right|^2\left|\frac{u_i}{H_i} - a_{\min 1}\right|^2 + \sum_{i=1}^{L}\left|H_i\right|^2\left|\frac{u_i}{H_i} - a_{\min 0}\right|^2 \\ &= -\sum_{i=1}^{L}\left|u_i - a_{\min 1}H_i\right|^2 + \sum_{i=1}^{L}\left|u_i - a_{\min 0}H_i\right|^2 \\ &= \sum_{i=1}^{L}[2\cdot \mathrm{Re}\{u_i {a_{\min 1}}^* {H_i}^*\} - \left|a_{\min 1}H_i\right|^2] - \sum_{i=1}^{L}[2\cdot \mathrm{Re}\{u_i {a_{\min 0}}^* {H_i}^*\} - \left|a_{\min 0}H_i\right|^2] \\ &= 2\sum_{i=1}^{L}\mathrm{Re}\{u_i(a_{\min 1} - a_{\min 0})^* {H_i}^*\} - \{\left|a_{\min 1}\right|^2 - \left|a_{\min 0}\right|^2\}\sum_{i=1}^{L}\left|H_i\right|^2 . \end{aligned} \qquad (7)$$

In expression (7), u_iH_i has been substituted for r_i. In this manner, each observation is weighted with the complex-conjugate of the channel response H_i for the corresponding antenna. Hence, by incorporation of the channel response H_i, equalization can be performed jointly with the soft-demapping function, as discussed in further detail below. Finally, the soft decision can be defined as the scaled log likelihood:

$$\begin{aligned} \Lambda(b_l) &\equiv \frac{\sigma_n^2}{2}\cdot LLR(b_l) \\ &\approx \frac{1}{2}\sum_{i=1}^{L}\mathrm{Re}\{u_i(a_{\min 1} - a_{\min 0})^* {H_i}^*\} - \frac{1}{4}\{\left|a_{\min 1}\right|^2 - \left|a_{\min 0}\right|^2\}\sum_{i=1}^{L}\left|H_i\right|^2 . \end{aligned} \qquad (8)$$

Note that, in expressions (7) and (8), computation of the log likelihood to generate a soft decision is based on the unequalized observation sample u_i. The frequency

equalization, which is essentially an act of dividing u_i by the channel response H_i for the pertinent frequency bin, is implicit in expression (7) above. In this sense, expressions (7) and (8) represent a joint equalization and soft-demapping operation. In other words, equalization and soft-demapping can be performed jointly, rather than independently, using a common set of demapping functions that implicate equalization. Advantageously, this feature may enable the sharing of hardware and processing overhead, thereby reducing size, complexity and cost within the wireless receiver components of wireless communication device 16.

[0048] The branch metric in the soft Viterbi algorithm used for decoding can be obtained by simply summing the M consecutive soft decisions, after appropriate deinterleaving, as represented by the expression:

$$\lambda(b_1'b_2'\cdots b_M') = \sum_{l=1}^{M}\left(b_l' - \frac{1}{2}\right)\Lambda(b_l') \tag{9}$$

where b_l' represents deinterleaved bits. Note that arbitrary scaling of the log likelihood ratio does not affect the Viterbi decoding operation as long as the scaling is consistent over the entire bit sequence. This particular scaling of the log likelihood expression (8) may be chosen because it tends to simplify the final expression. In addition, the log likelihood (8) without the scaling may improve the dynamic range utilization in the finite precision implementation.

[0049] FIGS. 3-6 are graphs illustrating typical gray-coded QAM constellations that may be used for QAM symbol coding in accordance with various embodiments of the invention. FIG. 3, for example, illustrates a BPSK symbol constellation. FIG. 4 represents a symbol constellation for 4-QAM coding, FIG. 5 represents a symbol constellation for 16-QAM coding, and FIG. 6 represents a symbol constellation for 64-QAM coding. For higher order QAM coding, such as 256-QAM and 1024-QAM, signal constellations are tabulated in Tables 1 and 2, respectively, below.

TABLE 1
256-QAM Mapping

Coded bits (b_1, b_2, b_3, b_4)	Real part	Coded bits (b_5, b_6, b_7, b_8)	Imaginary part
0000	-15	0000	-15
0001	-13	0001	-13
0011	-11	0011	-11
0010	-9	0010	-9
0110	-7	0110	-7
0111	-5	0111	-5
0101	-3	0101	-3
0100	-1	0100	-1
1100	1	1100	1
1101	3	1101	3
1111	5	1111	5
1110	7	1110	7
1010	9	1010	9
1011	11	1011	11
1001	13	1001	13
1000	15	1000	15

TABLE 2
1024-QAM Mapping

Coded bits (b_1, b_2, b_3, b_4, b_5)	Real part	Coded bits (b_6, b_7, b_8, b_9, b_{10})	Imaginary part
00000	-31	00000	-31
00001	-29	00001	-29
00011	-27	00011	-27
00010	-25	00010	-25
00110	-23	00110	-23
00111	-21	00111	-21
00101	-19	00101	-19
00100	-17	00100	-17
01100	-15	01100	-15
01101	-13	01101	-13
01111	-11	01111	-11
01110	-9	01110	-9
01010	-7	01010	-7
01011	-5	01011	-5
01001	-3	01001	-3
01000	-1	01000	-1
11000	1	11000	1
11001	3	11001	3
11011	5	11011	5
11010	7	11010	7
11110	9	11110	9
11111	11	11111	11
11101	13	11101	13
11100	15	11100	15
10100	17	10100	17
10101	19	10101	19
10111	21	10111	21
10110	23	10110	23
10010	25	10010	25
10011	27	10011	27
10001	29	10001	29
10000	31	10000	31

Coded bits are mapped to the real and imaginary components of a QAM symbol independently. For example, for 64-QAM, the first three bits (b_1, b_2, b_3) determine the real part of the QAM symbol and the remaining three bits (b_4, b_5, b_6) determine the imaginary part of the QAM symbol. With this type of Gray-coded QAM, the boundary lines that separate the QAM symbols associated with $b_l = 1$ from those associated with $b_l = 0$, i.e., the inter-bit decision boundaries, are either horizontal or vertical, for any l. It can be further shown that when these decision boundaries are horizontal, the "nearest" symbols $a_{\min 1}$ and $a_{\min 0}$, for purposes of expressions (3) and (4) above, share a common real (horizontal) component, and differ only in their imaginary components. Likewise, when the boundaries are vertical, $a_{\min 1}$ and $a_{\min 0}$ share the same imaginary (vertical) component.

[0050] Advantageously, the soft demapping technique may be based on a subset of the transmitted symbol constellation for reduced complexity. It can be seen that in expression (8) above, advantageously, the soft decision $\Lambda(b_l)$ is given as a piece-wise linear function of either $\sum_{i=1}^{L} \mathrm{Re}\{u_i H_i^*\}$ or $\sum_{i=1}^{L} \mathrm{Im}\{u_i H_i^*\}$. Thus, the soft-demapping technique may apply piecewise linear functions based on the real and imaginary components of the combined observation and on the combined energy of the channel responses. For a given bit b_l, the absolute value of the slope of the function $\Lambda(b_l)$ can change as a function of $\sum_{i=1}^{L} \mathrm{Re}\{u_i H_i^*\}$ or $\sum_{i=1}^{L} \mathrm{Im}\{u_i H_i^*\}$.

[0051] A further complexity-reducing approximation can be made to expression (8) by confining $a_{\min 1}$ and $a_{\min 0}$ to be near the boundary lines. When the "nearest" symbols $a_{\min 1}$ and $a_{\min 0}$ are chosen only from the symbols closest to the nearest boundary line, the absolute value of the slope in $\Lambda(b_l)$ remains fixed for a given bit b_l, further reducing implementation complexity. Thus, the soft demapping rules may be based on minimum distance symbols $a_{\min 1}$ and $a_{\min 0}$ associated with pertinent bit values in the transmitted symbol.

[0052] For an illustrative example, consider 16-QAM coding and two receive antennas, as shown in the example of FIG. 2. In the constellations shown in FIG. 5, the boundary line that separates the symbols associated with $b_1 = 1$ from the symbols

associated with $b_1 = 0$ is the vertical line through the origin. Since the boundary is vertical, the imaginary (vertical) components of $a_{\min 1}$ and $a_{\min 0}$ are identical and thus do not play a role. Consequently, focusing on the symbols near the boundary, it is possible to simply set $a_{\min 1} = 1$ and $a_{\min 0} = -1$. Substituting these values in expression (8), letting

$$d_I = \sum_{i=1}^{2} \mathrm{Re}\{u_i^* H_i^*\} \tag{10}$$

and ignoring the approximation, expression (8) can be rewritten as:

$$\Lambda(b_1) = d_I. \tag{11}$$

This soft decision rule is illustrated for b_1 in FIG. 7 for the 16-QAM case. For the second bit b_2, the boundaries are formed at +2 and –2, as also shown in FIG. 7. For the region close to the +2 boundary, i.e., when $d_I > 0$, we can set $a_{\min 1} = +1$ and $a_{\min 0} = +3$, again ignoring the imaginary components. For the region close to the -2 boundary, i.e., when $d_I < 0$, we can set $a_{\min 1} = -1$ and $a_{\min 0} = -3$. Expression (8) then reduces to:

$$\Lambda(b_2) = \begin{cases} -d_I + 2P & \text{for } d_I > 0 \\ d_I + 2P & \text{for } d_I < 0 \end{cases} \tag{12}$$

where

$$P = \sum_{i=1}^{2} |H_i|^2 . \tag{13}$$

The boundary line for b_3 is formed as the horizontal line through the origin. The nearest symbols around the boundary are $a_{\min 1} = +j$ and $a_{\min 0} = -j$, ignoring the common real component. Substituting these values in expression (8) and letting:

$$d_Q = \sum_{i=1}^{2} \mathrm{Im}\{u_i^* H_i^*\}, \tag{14}$$

the following is obtained:

$$\Lambda(b_3) = d_Q. \tag{15}$$

Following similar steps, it is possible to obtain:

$$\Lambda(b_4)=\begin{cases}-d_Q+2P & \text{for } d_Q>0\\ d_Q+2P & \text{for } d_Q<0.\end{cases} \tag{16}$$

A similar soft decision rule can be applied for a single antenna case with an equalized signal. For reduced complexity, the minimum distance symbols can be further confined to be within a predetermined distance of an inter-symbol decision boundary. If the nearest symbols are not confined close to the boundary, a somewhat more complicated but slightly improved soft decision rule for the first bit can be obtained as follows:

$$\Lambda(b_1)=\begin{cases}d_I & \text{for } |d_I|<2P\\ 2d_I-2P & \text{for } d_I\geq 2P\\ -2d_I+2P & \text{for } d_I<2P\end{cases} \tag{17}$$

where $a_{\min 1}=+3$ and $a_{\min 0}=-1$ for the second region, and $a_{\min 1}=-3$ and $a_{\min 0}=+1$ for the third region. Similarly, for the third bit b_3, a soft decision rule can be obtained as follows:

$$\Lambda(b_3)=\begin{cases}d_Q & \text{for } |d_Q|<2P\\ 2d_Q-2P & \text{for } d_Q\geq 2P\\ -2d_Q+2P & \text{for } d_Q<2P\end{cases} \tag{18}$$

where the nearest symbols are set as $a_{\min 1}=+3j$ and $a_{\min 0}=-j$ for the second region and $a_{\min 1}=-3j$ and $a_{\min 0}=j$ for the third region. Following the same steps, the soft decisions for 64-QAM can be obtained as shown in Fig. 8. In the above examples, it is noted that the soft decision for a subsequently computed bit, bit n, may computed recursively from the previously computed soft decision, bit n-1.

[0053] FIG. 9 is a block diagram illustrating a soft demapping unit 28 for BPSK encoding, the lowest order form of QAM encoding. Soft demapping unit 28 may be configured to apply soft decision rules as described above. Although the example of FIG. 9 pertains to a wireless communication device 16 having two receive antennas 18A, 18B for receive diversity, the invention can be readily extended to an arbitrary number of multiple antennas. As shown in FIG. 9, first and second FFT units 30A, 30B receive first and second RF signals $R_{1,j,k}$ and $R_{2,j,k}$ from antennas 18A, 18B,

respectively. FFT units 30A, 30B demodulate the incoming RF signals $R_{1,j,k}$ and $R_{2,j,k}$ to produce FFT outputs that provide demodulated signals $u_{1,k}$ and $u_{2,k}$, respectively.

[0054] For BPSK in the example of FIG. 9, the soft decision is simply:

$$\Lambda(b_1) = d_I . \tag{19}$$

[0055] Within soft demapper unit 28, multipliers 36A, 36B equalize demodulated signals $u_{1,k}$ and $u_{2,k}$ with channel gain coefficients $H^*_{1,k}$ and $H^*_{2,k}$, respectively. A signal combiner 38 combines the equalized signals produced by multipliers 36A, 36B. Element 40 extracts the real component of the combined signal and applies rules as described above to produce a soft decision $\Lambda(b_1)$. The soft decision $\Lambda(b_1)$ is applied to a de-interleaver 32, which produces a de-interleaved soft decision that can be used to compute branch metrics for use in a Viterbi convolutional decoder 34.Notably, there is no need for separate hardware for equalization and weighting by channel signal-to-noise ratio (SNR). Instead, equalization is integrated with the hardware used to perform the soft-demapping function. Accordingly, the OFDM demodulator (FFTs 34A, 34B), de-interleaver 30, and Viterbi decoder 32 are shown together in FIG. 9. For other mapping methods illustrated with respect to FIGS. 10-14 below, however, only the applicable soft demapper unit will be shown for brevity. In the examples of FIGS. 10-14, the FFT units 34A, 34B, de-interleaver 30, and Viterbi decoder 32 may be provided substantially as shown in FIG. 9.

[0056] FIG. 10 is a block diagram illustrating an exemplary soft demapping unit 42 for 4-QAM encoding. In 4-QAM mapping, the coded bits b_1 and b_2 are mapped to the real and imaginary parts, respectively, of a symbol, as follows:

$$\Lambda(b_1) = d_I \tag{20}$$

$$\Lambda(b_2) = d_Q . \tag{21}$$

FIG. 11 is a block diagram illustrating a soft demapping unit 44 for 16-QAM encoding. In 16-QAM mapping, the coded bit sequence (b_1, b_2) is mapped to the real part of a symbol and (b_3, b_4) to the imaginary part. The soft demapping technique may involve generating one or more soft decision bits indicative of the transmitted

symbol for a combined observation according to soft demapping rules that are based on a subset of the transmitted symbol constellation for reduced complexity, e.g., as described above with respect to expression (8). As will be described, the soft demapping rules may be based on the minimum distance symbols associated with pertinent bits in the transmitted symbol. A minimum distance symbol may refer to a symbol that is closest to a particular decision boundary. In addition, the minimum distance symbols can be further constrained to be near the pertinent decision boundary, i.e., within a predetermined distance of the decision boundary. As an illustration, for reduced complexity, the soft decisions can be determined according to piecewise decision rules as follows:

$$\Lambda(b_1) = d_I \tag{22}$$

$$\begin{aligned}\Lambda(b_2) &= \begin{cases} -d_I + 2P & \text{for } d_I > 0 \\ d_I + 2P & \text{for } d_I < 0 \end{cases} \\ &= -|\Lambda(b_1)| + 2P \end{aligned} \tag{23}$$

$$\Lambda(b_3) = d_Q$$

(24)

$$\begin{aligned}\Lambda(b_4) &= \begin{cases} -d_Q + 2P & \text{for } d_Q > 0 \\ d_Q + 2P & \text{for } d_Q < 0 \end{cases} \\ &= -|\Lambda(b_3)| + 2P \end{aligned} \tag{25}$$

[0057] FIG. 12 is a block diagram illustrating a soft demapping unit 46 for 64-QAM encoding. For 64-QAM, the coded bit sequence (b_1, b_2, b_3) is mapped to the real part of a symbol, and the coded bit sequence (b_4, b_5, b_6) is mapped to the imaginary part. The soft decisions can be represented by piecewise functions as follows:

$$\Lambda(b_1) = d_I \tag{26}$$

$$\begin{aligned}\Lambda(b_2) &= \begin{cases} -d_I + 4P & \text{for } d_I > 0 \\ d_I + 4P & \text{for } d_I < 0 \end{cases} \\ &= -|\Lambda(b_1)| + 4P \end{aligned} \tag{27}$$

$$\Lambda(b_3)=\begin{cases} d_I+6P & \text{for } d_I \le -4P \\ -d_I-2P & \text{for } -4P < d_I \le 0 \\ d_I-2P & \text{for } 0 < d_I \le 4P \\ -d_I+6P & \text{for } d_I > 4P \end{cases} \qquad (28)$$
$$=-|\Lambda(b_2)|+2P$$

$$\Lambda(b_4)=d_Q \qquad (29)$$

$$\Lambda(b_5)=\begin{cases} -d_Q+4P & \text{for } d_Q > 0 \\ d_Q+4P & \text{for } d_Q < 0 \end{cases} \qquad (30)$$
$$=-|\Lambda(b_4)|+4P$$

$$\Lambda(b_6)=\begin{cases} d_Q+6P & \text{for } d_Q \le -4P \\ -d_Q-2P & \text{for } -4P < d_Q \le 0 \\ d_Q-2P & \text{for } 0 < d_Q \le 4P \\ -d_Q+6P & \text{for } d_Q > 4P \end{cases} \qquad (31)$$
$$=-|\Lambda(b_5)|+2P$$

[0058] FIG. 13 is a block diagram illustrating a soft demapping unit 48 for 256-QAM encoding. In 256-QAM coding, the procedure described above with reference to FIG. 12 can be followed. The soft decisions for 256-QAM coding are represented as follows:

$$\Lambda(b_1)=d_I, \qquad (32)$$
$$\Lambda(b_2)=-|\Lambda(b_1)|+8P, \qquad (33)$$
$$\Lambda(b_3)=-|\Lambda(b_2)|+4P, \qquad (34)$$
$$\Lambda(b_4)=-|\Lambda(b_3)|+2P, \qquad (35)$$
$$\Lambda(b_5)=d_Q, \qquad (36)$$
$$\Lambda(b_6)=-|\Lambda(b_5)|+8P, \qquad (37)$$
$$\Lambda(b_7)=-|\Lambda(b_6)|+4P, \qquad (38)$$
$$\Lambda(b_8)=-|\Lambda(b_7)|+2P. \qquad (39)$$

[0059] FIG. 14 is a block diagram illustrating a soft demapping unit 50 for 1024-QAM encoding. In 1024-QAM coding, the soft decisions for 1024-QAM are represented as follows:

$$\Lambda(b_1)=d_I, \qquad (40)$$
$$\Lambda(b_2)=-|\Lambda(b_1)|+16P, \qquad (41)$$

$$\Lambda(b_3) = -|\Lambda(b_2)| + 8P, \quad (42)$$

$$\Lambda(b_4) = -|\Lambda(b_3)| + 4P, \quad (43)$$

$$\Lambda(b_5) = -|\Lambda(b_4)| + 2P, \quad (44)$$

$$\Lambda(b_6) = d_Q, \quad (45)$$

$$\Lambda(b_7) = -|\Lambda(b_6)| + 16P, \quad (46)$$

$$\Lambda(b_8) = -|\Lambda(b_7)| + 8P, \quad (47)$$

$$\Lambda(b_9) = -|\Lambda(b_8)| + 4P, \quad (48)$$

$$\Lambda(b_{10}) = -|\Lambda(b_9)| + 2P. \quad (49)$$

[0060] A phase error estimator for a wireless communication device incorporating a receive diversity arrangement as described herein will now be discussed. An OFDM receiver typically uses a single clock source to derive all necessary clocks for carrier recovery and sampling of a received signal. Similarly, clocks for an OFDM transmitter are typically derived from a single clock source. In this case, the phase errors existing both in the carrier and the sampler will not change over the diversity paths. Including the carrier and sampling phase errors, the demodulated signal (observation sample) $u_{i,n}$ at the output of the FFT unit in an OFDM system can be represented by:

$$u_{i,n} = S_n \cdot H_{i,n} \cdot e^{j(n\Delta\phi_s + \Delta\phi_c)} + N'_{i,n}, \quad (50)$$

where S_n, $-N/2 \le n \le N/2$, is the transmitted symbol through the nth sub-carrier, $H_{i,n}$, $1 \le i \le L$, is the channel response of the nth sub-carrier and the ith diversity path, $j = \sqrt{-1}$, $\Delta\phi_c$ is the carrier phase error, $\Delta\phi_s$ is the sampler phase error, and $N'_{i,n}$ is the phase rotated noise sample. Note that in expression (50), only one symbol is considered. The phase errors $\Delta\phi_c$ and $\Delta\phi_s$ remain the same in different receive diversity paths.

[0061] Multiplying both sides of expression (50) by $S_n^* \cdot H_{i,n}^*$ and summing the results over the diversity paths results in

$$\sum_{i=1}^{L} u_{i,n} \cdot S_n^* \cdot H_{i,n}^* = e^{j(n\Delta\phi_s + \Delta\phi_c)} \sum_{i=1}^{L} |S_n \cdot H_{i,n}|^2 + \sum_{i=1}^{L} N''_{i,n}, \quad (51)$$

where $N''_{i,n} = N'_{i,n} \cdot S^*_n \cdot H^*_{i,n}$. In accordance with the invention, the phase error estimator can share hardware used for the soft demapper unit of the Viterbi algorithm. From expression (51), the phase error can be estimated as:

$$n\Delta\phi_s + \Delta\phi_c = angle\left(\sum_{i=1}^{L} u_{i,n} \cdot H^*_{i,n} \cdot S^*_n\right). \qquad (52)$$

The estimates of the channel response and transmitted symbol based on the received signal can be used for $H_{i,n}$ and S_n, respectively, if these are not known to the receiver. The phase error is typically so small that the angle in (52) can be approximated by the division of the imaginary part of the argument by the real part as:

$$n\Delta\phi_s + \Delta\phi_c = \frac{\mathrm{Im}\left(\sum_{i=1}^{L} u_{i,n} \cdot H^*_{i,n} \cdot S^*_n\right)}{\mathrm{Re}\left(\sum_{i=1}^{L} u_{i,n} \cdot H^*_{i,n} \cdot S^*_n\right)}. \qquad (53)$$

Each component of the phase errors can be estimated by averaging expression (53) throughout the sub-carriers as represented below:

$$\Delta\phi_c = \frac{1}{(N/2)} \sum_{n=1}^{N/2} \left(\frac{\mathrm{Im}\left(\sum_{i=1}^{L} u_{i,n} \cdot H^*_{i,n} \cdot S^*_n\right)}{\mathrm{Re}\left(\sum_{i=1}^{L} u_{i,n} \cdot H^*_{i,n} \cdot S^*_n\right)} + \frac{\mathrm{Im}\left(\sum_{i=1}^{L} u_{i,-n} \cdot H^*_{i,-n} \cdot S^*_{-n}\right)}{\mathrm{Re}\left(\sum_{i=1}^{L} u_{i,-n} \cdot H^*_{i,-n} \cdot S^*_{-n}\right)} \right) \quad \text{and} \quad (54)$$

$$\Delta\phi_s = \frac{1}{(N/2+1)(N/2)} \sum_{n=1}^{N/2} \left(\frac{\mathrm{Im}\left(\sum_{i=1}^{L} u_{i,n} \cdot H^*_{i,n} \cdot S^*_n\right)}{\mathrm{Re}\left(\sum_{i=1}^{L} u_{i,n} \cdot H^*_{i,n} \cdot S^*_n\right)} - \frac{\mathrm{Im}\left(\sum_{i=1}^{L} u_{i,n-N/2-1} \cdot H^*_{i,n-N/2-1} \cdot S^*_{n-N/2-1}\right)}{\mathrm{Re}\left(\sum_{i=1}^{L} u_{i,n-N/2-1} \cdot H^*_{i,n-N/2-1} \cdot S^*_{n-N/2-1}\right)} \right)$$

. (55)

The above averaging (summation) of the phase errors associated with an individual sub-carrier can be made selective in order to save hardware or reduce the latency involved in the phase error calculation. In particular, if there are known transmitted symbols such as pilot tones, the phase errors of these tones can be used in the calculation of the phase errors.

[0062] The phase error estimation in expression (55) does not need to consider the channel SNR associated with the sub-carrier and diversity path. Assuming the channel noise is additive white Gaussian, the SNR of the sub-carrier n of the ith diversity path is proportional to $|H_{i,n}|^2$. The combined SNR over the diversity paths is also proportional to $\sum_{i=1}^{L}|H_{i,n}|^2$. The performance of the phase error estimator represented in expressions (54) and (55) can be improved by weighting individual phase error estimates by the combined SNR as represented below:

$$\Delta\phi_c = \frac{1}{(N/2)\cdot sumw}\sum_{n=1}^{N/2}\left(\frac{\mathrm{Im}\left(\sum_{i=1}^{L}u_{i,n}\cdot H_{i,n}^{*}\cdot S_{n}^{*}\right)}{\mathrm{Re}\left(\sum_{i=1}^{L}u_{i,n}\cdot H_{i,n}^{*}\cdot S_{n}^{*}\right)}\cdot\sum_{i=1}^{L}|H_{i,n}|^2+\frac{\mathrm{Im}\left(\sum_{i=1}^{L}u_{i,-n}\cdot H_{i,-n}^{*}\cdot S_{-n}^{*}\right)}{\mathrm{Re}\left(\sum_{i=1}^{L}u_{i,-n}\cdot H_{i,-n}^{*}\cdot S_{-n}^{*}\right)}\cdot\sum_{i=1}^{L}|H_{i,-n}|^2\right) \quad (56)$$

$$\Delta\phi_s = \frac{1}{(N/2+1)(N/2)\cdot sumw}\sum_{n=1}^{N/2}\left(\frac{\mathrm{Im}\left(\sum_{i=1}^{L}u_{i,n}\cdot H_{i,n}^{*}\cdot S_{n}^{*}\right)}{\mathrm{Re}\left(\sum_{i=1}^{L}u_{i,n}\cdot H_{i,n}^{*}\cdot S_{n}^{*}\right)}\cdot\sum_{i=1}^{L}|H_{i,n}|^2-\frac{\mathrm{Im}\left(\sum_{i=1}^{L}u_{i,n-N/2-1}\cdot H_{i,n-N/2-1}^{*}\cdot S_{n-N/2-1}^{*}\right)}{\mathrm{Re}\left(\sum_{i=1}^{L}u_{i,n-N/2-1}\cdot H_{i,n-N/2-1}^{*}\cdot S_{n-N/2-1}^{*}\right)}\cdot\sum_{i=1}^{L}|H_{i,n-N/2-1}|^2\right) \quad (57)$$

where $sumw=\sum_{n=-N/2,n\neq 0}^{N/2}\sum_{i=1}^{L}|H_{i,n}|^2$. Because pairs of sub-carrier phase errors are used to estimate the individual carrier and sampler phase error components, the weighting can be applied piece-wise as follows:

$$\Delta\phi_c = \frac{1}{(N/2)\cdot sumw_c}\sum_{n=1}^{N/2}\left(\frac{\mathrm{Im}\left(\sum_{i=1}^{L}u_{i,n}\cdot H_{i,n}^{*}\cdot S_{n}^{*}\right)}{\mathrm{Re}\left(\sum_{i=1}^{L}u_{i,n}\cdot H_{i,n}^{*}\cdot S_{n}^{*}\right)}+\frac{\mathrm{Im}\left(\sum_{i=1}^{L}u_{i,-n}\cdot H_{i,-n}^{*}\cdot S_{-n}^{*}\right)}{\mathrm{Re}\left(\sum_{i=1}^{L}u_{i,-n}\cdot H_{i,-n}^{*}\cdot S_{-n}^{*}\right)}\right)\cdot\min\left(\sum_{i=1}^{L}|H_{i,n}|^2,\sum_{i=1}^{L}|H_{i,-n}|^2\right) \quad (58)$$

$$\Delta\phi_s = \frac{1}{(N/2+1)(N/2)\cdot sumw_s}\sum_{n=1}^{N/2}\left(\frac{\mathrm{Im}\left(\sum_{i=1}^{L}u_{i,n}\cdot H_{i,n}^{*}\cdot S_{n}^{*}\right)}{\mathrm{Re}\left(\sum_{i=1}^{L}u_{i,n}\cdot H_{i,n}^{*}\cdot S_{n}^{*}\right)}-\frac{\mathrm{Im}\left(\sum_{i=1}^{L}u_{i,n-N/2-1}\cdot H_{i,n-N/2-1}^{*}\cdot S_{n-N/2-1}^{*}\right)}{\mathrm{Re}\left(\sum_{i=1}^{L}u_{i,n-N/2-1}\cdot H_{i,n-N/2-1}^{*}\cdot S_{n-N/2-1}^{*}\right)}\right)\cdot\min\left(\sum_{i=1}^{L}|H_{i,n}|^2,\sum_{i=1}^{L}|H_{i,n-N/2-1}|^2\right) \quad (59)$$

where $sumw_c = \sum_{n=1}^{N/2} \min\left(\sum_{i=1}^{L} |H_{i,n}|^2, \sum_{i=1}^{L} |H_{i,-n}|^2 \right)$ and

$sumw_s = \sum_{n=1}^{N/2} \min\left(\sum_{i=1}^{L} |H_{i,n}|^2, \sum_{i=1}^{L} |H_{i,n-N/2-1}|^2 \right)$.

[0063] The phase error is small under normal operating conditions. In this case, the imaginary part of $\sum_{i=1}^{L} u_{i,n} \cdot H_{i,n}^* \cdot S_n^*$ is much smaller than the real part. The phase error estimate proportional to the actual phase error can be obtained by the expression:

$$\Delta\phi_c = \frac{1}{(N/2) \cdot sumw_c} \sum_{n=1}^{N/2} \left(\mathrm{Im}\left(\sum_{i=1}^{L} u_{i,n} \cdot H_{i,n}^* \cdot S_n^* \right) + \mathrm{Im}\left(\sum_{i=1}^{L} u_{i,-n} \cdot H_{i,-n}^* \cdot S_{-n}^* \right) \right) \cdot \min\left(\sum_{i=1}^{L} |H_{i,n}|^2, \sum_{i=1}^{L} |H_{i,-n}|^2 \right) \quad (60)$$

$$\Delta\phi_s = \frac{1}{(N/2+1)(N/2) \cdot sumw_s} \sum_{n=1}^{N/2} \left(\mathrm{Im}\left(\sum_{i=1}^{L} u_{i,n} \cdot H_{i,n}^* \cdot S_n^* \right) - \mathrm{Im}\left(\sum_{i=1}^{L} u_{i,n-N/2-1} \cdot H_{i,n-N/2-1}^* \cdot S_{n-N/2-1}^* \right) \right) \cdot \min\left(\sum_{i=1}^{L} |H_{i,n}|^2, \sum_{i=1}^{L} |H_{i,n-N/2-1}|^2 \right) \quad (61)$$

[0064] In effect, the carrier phase error $\Delta\phi_c$ can be estimated by removing the sampling phase error component and averaging the residual subcarrier phase errors. The phase shift magnitude of the subcarrier 'n' due to the sampling phase error is the same amount as for the complementary subcarrier '-n,' i.e., the complementary subcarrier. However, the signs of the phase shift for the complementary pair of subcarriers 'n' and '-n' are opposite. By adding the two subcarrier phase errors corresponding to the complementary subcarriers 'n' and '-n', the phase shift due to the sampling phase error can be removed.

[0065] Also, the sampling phase error $\Delta\phi_s$ can be estimated by removing the carrier phase error component and averaging the residual subcarrier phase errors. The phase shift due to the carrier phase error is the same throughout the subcarriers. By taking

the difference of any two subcarrier phase errors, the phase shift due to the carrier phase error can be removed. To obtain the largest residual phase error after taking the difference, the two subcarriers taken for the difference should be separated by the greatest extent. For the subcarriers indexed in the range of [-N/2, N/2], the complementary pairs of subcarriers can be formed as (-N/2, 1), (-N/2+1,2), ..., (-1, N/2), where each pair has the index difference of N/2+1.

[0066] In the above phase error estimation expressions (56), (57), (58), (59), (60), and (61), the weighting factors can be quantized to reduce hardware complexity. For example, the weighting factors $\sum_{i=1}^{L}|H_{i,n}|^2$ for varying n can be quantized to values nearest to the power of 2 value. The estimation expressions (54) and (55) can also be modified to:

$$\Delta\phi_c = \frac{1}{(N/2)}\sum_{n=1}^{N/2}\left(\mathrm{Im}\left(\sum_{i=1}^{L}u_{i,n}\cdot H_{i,n}^{*}\cdot S_n^{*}\right)+\mathrm{Im}\left(\sum_{i=1}^{L}u_{i,-n}\cdot H_{i,-n}^{*}\cdot S_{-n}^{*}\right)\right) \quad (62)$$

$$\Delta\phi_s = \frac{1}{(N/2+1)(N/2)}\sum_{n=1}^{N/2}\left(\mathrm{Im}\left(\sum_{i=1}^{L}u_{i,n}\cdot H_{i,n}^{*}\cdot S_n^{*}\right)-\mathrm{Im}\left(\sum_{i=1}^{L}u_{i,n-N/2-1}\cdot H_{i,n-N/2-1}^{*}\cdot S_{n-N/2-1}^{*}\right)\right) \quad (63)$$

[0067] The performance of the phase error detector can be improved further by incorporating the power of the transmitted signal S_n in the averaging process. To examine the noise effect on the accuracy of the phase error estimate for varying transmitted signal power, assume that the channel responses and noises are the same for two observed signals, $u_{i,n}$ and $u_{i,m}$, the phase error is zero, and that only the transmitted signals are different. In particular, $H_{i,n}=H_{i,m}$, $N'_{i,n}=N'_{i,m}$, $\Delta\phi_s=\Delta\phi_c=0$, and $S_n\neq S_m$. Then, for $|S_n|>|S_m|$, the following relationship between the calculated phase errors always holds for the two subcarriers:

$$angle(u_{i,n})-angle(H_{i,n})-angle(S_n)\leq angle(u_{i,m})-angle(H_{i,m})-angle(S_m). \quad (64)$$

Assuming that $H_{i,n}=H_{i,m}$, expression (64) reduces to:

$$angle(u_{i,n}) - angle(S_n) \le angle(u_{i,m}) - angle(S_m). \quad (65)$$

Without the loss of the generality, we can assume that $angle(S_n) = angle(S_m)$. Then, expression (65) reduces to:

$$angle(u_{i,n}) \le angle(u_{i,m}). \quad (66)$$

Since the magnitude of $S_n \cdot H_{i,n}$ for the first signal is larger than that of $S_m \cdot H_{i,m}$ for the second signal, for the same noise $N'_{i,n} = N'_{i,m}$, the above relationship (66) always holds. In conclusion, the smaller the transmitted signal power is, the more susceptible the phase estimate is to the noise.

[0068] To improve the phase error estimate under the noisy channel condition, those transmitted signals with small power can be removed from the phase error calculation. This can simply be implemented by setting the estimated transmitted signal S_n to zero if it has a small power. As an example, for the 256 QAM case, if the estimated transmitted signal S_n is one of $\{(i,j) \mid i \in \{\pm 1, \pm 3\}$ and $j \in \{\pm 1, \pm 3\}\}$, then the estimate is set to $S_n = 0$. Similarly, for the 64 QAM case, the estimated transmitted signal S_n is set to 0 if it is one of $\{(1,1), (1,-1), (-1,1), (-1,-1)\}$. The angle operator should output a zero angle for the zero input for both the real part and the imaginary part. With these settings, both 64QAM and 256QAM coding do not use 6.25% of the signal constellation points in the phase error calculation.

[0069] According to the IEEE 802.11a standard, four pilot tones are modulated by BPSK. The pilot tones are not affected by the implementation described herein. For IEEE 802.11a applications, even in the extreme situation where none of the transmitted signals are used in the phase error calculation due to small power levels, there are at least four pilot tones used for the phase error calculation. Furthermore, the probability of transmitting all of the signals with small power levels is very low.

[0070] FIG. 15 is a block diagram illustrating a phase locked loop 55 with frequency domain correction in accordance with an embodiment of the invention. As shown in FIG. 15, phase locked loop 55 includes multiple sampling and demodulation paths corresponding to the multiple signals $R_{1,j,k}$ and $R_{2,j,k}$ received via the receive diversity antennas 18A, 18B. Digital phase locked loop 55 demodulates each signal in portions or blocks. A sampler (not shown in FIG. 15) separates the blocks in each

signal $R_{1,j,k}$ and $R_{2,j,k}$ for demodulation. The sampler typically includes an analog-to-digital converter that transforms each of the received analog carrier signals into a digital carrier signal.

[0071] The sampler takes a plurality of samples of the respective time-domain signals $R_{1,j,k}$ and $R_{2,j,k}$ during a sampling window 56, 58, respectively. Sampling window 56, 58 remains "open" for a discrete period of time, during which a fixed number of samples of the received time-domain signal can be taken at a particular sampling rate. The duration between samples is the "sampling period," and the sum of all sampling periods equals the duration of respective sampling window 56, 58. The lengths of the sampling periods are controlled by a sampling clock, which also determines the sampling rate. The sampling clock can be advanced or delayed as will be described below.

[0072] The signal sampled in each window 56, 58 defines a sequence that is passed to a respective fast Fourier transform (FFT) unit 60, 62 for processing in the frequency domain. In the example of FIG. 15, phase correction blocks 68, 70 multiply the received signals by $e^{-j\left(n\hat{\phi}_s+\hat{\phi}_c\right)}$, where $\hat{\phi}_s$ and $\hat{\phi}_c$ are the lowpass filtered and accumulated phase error estimates $\Delta\phi_s$ and $\Delta\phi_c$, respectively. Hence, each phase correction block 68, 70 performs two distinct forms of phase correction for subsequent observation samples based on estimated phase error. One form of phase error is carrier phase error, $\Delta\phi_c$, which results from discrepancy between the transmitter carrier frequency and the free-running oscillator frequency of the receiver. Carrier phase error affects demodulation of all signals that may be carried by the carrier, and affects the signals equally. A second form of phase error is sampling phase error, $\Delta\phi_s$, which results from discrepancy between sampling frequencies of the transmitter and receiver. Sampling phase error does not affect all signals equally. Rather, the amount of sampling phase error depends upon the sub-carrier bin of the signal to be recovered.

[0073] To compensate for sampling phase error, $\Delta\phi_s$, each phase correction block 68, 70 multiplies the input signal by $e^{-j\left(n\hat{\phi}_s\right)}$ to adjust the respective sampling window 56, 58. When the sampling phase to be corrected is larger than π or smaller than $-\pi$, the window position is shifted backward or forward, respectively, by one sample and the phase to be corrected is added by -2π or 2π, respectively. To compensate

for carrier phase error, $\Delta\phi_c$, phase correction block 68, 70 multiplies the input signal by $e^{-j(\hat{\phi}_c)}$. A phase error estimator 74 generates phase error values $\Delta\phi_c$ and $\Delta\phi_s$. Loop filters 76, 78 have lowpass characteristics to remove the fast varying phase error components of phase error values $\Delta\phi_c$ and $\Delta\phi_s$, respectively.

[0074] Voltage controlled oscillators (VCO) 80, 82 receive the filtered output signals from loop filters 76, 78, respectively. Loop filters 76, 78 and VCO elements 80, 82 act independently, but may operate in a substantially similar fashion. The loop filter/VCO elements 50 and 54, respectively, receive an estimated instantaneous carrier phase error, denoted $\Delta\hat{\phi}_c$, and an estimated instantaneous sampling phase error (58), denoted $\Delta\hat{\phi}_s$, from phase error estimator 74. VCOs 80, 82 serve as digital emulators of the analog counterparts, which perform accumulation of input signals, and apply low pass filter and accumulated phase error signals $\hat{\phi}_s$ and $\hat{\phi}_c$ to phase correction blocks 68, 70.

[0075] Channel estimation blocks 64, 66 provide estimates of the channel response for each transmission channel carrying signals $R_{1,j,k}$ and $R_{2,j,k}$, respectively. Branch metric calculator 72 generates soft decision output codes $\Lambda(b_l - bn)$ based on the phase corrected sequences generated by phase correction blocks 68, 70, and the channel estimation values produced by channel estimators 64, 66. A slicer block 84 generates hard decisions based on the transmitted coded bits produced by branch metric calculator 72. Mapping block 86 then translates a finite number of bits from the coded bits to a transmitted symbol. Thus, the output of mapping block 86 is the estimate of the transmitted symbol. Phase error estimator 74 receives the estimated transmitted symbol from mapping element 86 and the joint phase corrected and equalized signal u*H from branch metric calculator 72, and produces sampling and carrier phase error values $\Delta\phi_c$ and $\Delta\phi_s$. Hence, phase error estimator 74 can be referred to as a soft decision-directed phase error estimator in the sense that it is responsive to the output of branch metric calculator 72. The structure and function of phase error estimator 74 will be described in greater detail below.

[0076] As mentioned above, loop filter 76 and VCO 80, which track sampling phase error, may include additional functionality. In particular, loop filter 76 and VCO 80 can be constructed to include window adjustment circuitry that applies the

estimated sampling phase error $\hat{\phi}_s$ to adjust windows 56, 58. When $\hat{\phi}_s$ is larger than π radians or smaller than $-\pi$ radians, advance/delay signals 83 are generated to adjust sampling windows 56, 58. When $\hat{\phi}_s$ is larger than π, windows 56, 58 are lagged by one sampling period, and $\hat{\phi}_s$ is set to $-2\pi+\hat{\phi}_s$. When $\hat{\phi}_s$ is smaller than $-\pi$, windows 56, 58 are adjusted in the other direction by one sampling period and $\hat{\phi}_s$ is set to $2\pi+\hat{\phi}_s$. In this way, $\hat{\phi}_s$ remains between $-\pi$ radians and π radians.

[0077] The number of samples taken in sampling windows 56, 58 remains unchanged, but the windows are advanced or delayed by one sampling period with each adjustment. In other words, window adjustment is performed in the time domain. The sampler may include an increment/decrement controller that responds to advance/delay signal 83. Notably, window adjustment is performed when needed to keep $\hat{\phi}_s$ between $-\pi$ radians and π radians, and is not necessarily performed after each sampling. Because the effect of the window adjustments is observed at the input of phase correction elements 68, 70 with some time delay associated with FFTs 60, 62, the sampling phase error estimate supplied to phase correction elements 68, 70 may be adjusted with the same delay to either $-2\pi+\hat{\phi}_s$ or $2\pi+\hat{\phi}_s$.

[0078] FIG. 16 is a block diagram illustrating an alternative phase locked loop 88 with time and frequency domain correction. Phase locked loop 88 conforms substantially to phase locked loop 55 of FIG. 15. However, the carrier and sampling phase error correction features are decoupled. In particular, phase error estimator 74 is configured as in FIG. 15 to produce a sampling phase error value $\Delta\phi_s$ and a carrier phase error value $\Delta\phi_c$. However, loop filter 78 and VCO 82 feed the low pass filtered carrier phase error value $\hat{\phi}_c$ to independent carrier phase estimation blocks 90, 92 that precede the sampler for each receive diversity path. In this manner, the incoming signals $R_{1,j,k}$ and $R_{2,j,k}$ are corrected for carrier phase error prior to sampling in windows 56, 58 and demodulation by FFTs 60, 62, providing a phase error correction in the time domain. Loop filter 76 and VCO 80 then feed the sampling phase error $\hat{\phi}_s$ to sampling phase correction blocks 68, 70, as well as advance/delay signals 83 to adjust sampling windows 56, 58.

[0079] FIG. 17 is a block diagram illustrating implementation of phase error estimators performing calculations as represented in expressions (54) and (55) above. A 16-QAM embodiment will be described herein to illustrate a joint implementation of a soft demapper and a phase error estimator. As shown in FIG. 17, a soft demapper unit 48 for 16-QAM (FIG. 11) is integrated with a set of elements forming a phase error estimator 74. Again, the exemplary implementation of phase error estimator 74 in FIG. 17 is designed to implement the phase error estimations of expressions (54) and (55). To that end, slicer block 84 includes sign comparators for 16-QAM soft decisions $\Lambda(b_1)$, $\Lambda(b_2)$, $\Lambda(b_3)$ and $\Lambda(b_4)$.

[0080] A 16-QAM mapping unit 86 maps the hard decisions from slicer block 84 to produce a transmitted symbol. Following the complex conjugate operation (94), the transmitted symbol is multiplied with the combined demodulated and equalized signal u/H and applied to phase error estimator 74. Phase error estimator 74, as shown in FIG. 17, extracts the real and imaginary components of the resulting u^*H signal and implements the calculations set forth in expressions (54) and (55) to produce carrier phase error $\Delta\hat{\phi}_c$ and sampling phase error $\Delta\hat{\phi}_s$. With phase error estimator 74 implemented as shown in FIG. 17, each component of the phase errors can be estimated throughout the sub-carriers as represented below:

$$\Delta\phi_c = \frac{1}{(N/2)}\sum_{n=1}^{N/2}\left(\frac{\mathrm{Im}\left(\sum_{i=1}^{L} u_{i,n}\cdot H_{i,n}^{*}\cdot S_{n}^{*}\right)}{\mathrm{Re}\left(\sum_{i=1}^{L} u_{i,n}\cdot H_{i,n}^{*}\cdot S_{n}^{*}\right)}+\frac{\mathrm{Im}\left(\sum_{i=1}^{L} u_{i,-n}\cdot H_{i,-n}^{*}\cdot S_{-n}^{*}\right)}{\mathrm{Re}\left(\sum_{i=1}^{L} u_{i,-n}\cdot H_{i,-n}^{*}\cdot S_{-n}^{*}\right)}\right) \quad \text{and} \quad (54)$$

$$\Delta\phi_s = \frac{1}{(N/2+1)(N/2)}\sum_{n=1}^{N/2}\left(\frac{\mathrm{Im}\left(\sum_{i=1}^{L} u_{i,n}\cdot H_{i,n}^{*}\cdot S_{n}^{*}\right)}{\mathrm{Re}\left(\sum_{i=1}^{L} u_{i,n}\cdot H_{i,n}^{*}\cdot S_{n}^{*}\right)}-\frac{\mathrm{Im}\left(\sum_{i=1}^{L} u_{i,n-N/2-1}\cdot H_{i,n-N/2-1}^{*}\cdot S_{n-N/2-1}^{*}\right)}{\mathrm{Re}\left(\sum_{i=1}^{L} u_{i,n-N/2-1}\cdot H_{i,n-N/2-1}^{*}\cdot S_{n-N/2-1}^{*}\right)}\right)$$

. (55)

[0081] FIG. 18 is a block diagram illustrating implementation of a phase error estimator 74' performing calculations as indicated in expressions (58) and (59) above. Phase error estimator 74' conforms substantially to phase error estimator 74 of FIG. 17, and is provided for a 16-QAM example. However, phase error estimator 74' further includes a quantizer block 96 that quantizes the weight of $|H_{i,k}|^2 + |H_{2,k}|^2$ to the

nearest power of two value. Quantization can help to reduce hardware complexity.

Min carrier block 98 calculates:

$$\min\left(quantize\left(\sum_{i=1}^{L}\left|H_{i,n}\right|^2\right), quantize\left(\sum_{i=1}^{L}\left|H_{i,-n}\right|^2\right)\right) \text{ for } 1 \le n \le \frac{N}{2}.$$

Min sampler block 100 calculates:

$$\min\left(quantize\left(\sum_{i=1}^{L}\left|H_{i,n}\right|^2\right), quantize\left(\sum_{i=1}^{L}\left|H_{i,n-N/2-1}\right|^2\right)\right) \text{ for } 1 \le n \le \frac{N}{2}.$$

Sum carrier block 102 and sum sampler block 104 calculate:

$$\sum_{n=1}^{N/2}\min\left(quantize\left(\sum_{i=1}^{L}\left|H_{i,n}\right|^2\right), quantize\left(\sum_{i=1}^{L}\left|H_{i,-n}\right|^2\right)\right) \text{ and}$$

$$\sum_{n=1}^{N/2}\min\left(quantize\left(\sum_{i=1}^{L}\left|H_{i,n}\right|^2\right), quantize\left(\sum_{i=1}^{L}\left|H_{i,n-N/2-1}\right|^2\right)\right), \text{ respectively.}$$

The carrier and sampler blocks 98, 100, 102, 104 provide additional inputs that enable phase error estimator 74' to perform the calculations in expressions (58) and (59) as indicated below:

$$\Delta\phi_c = \frac{1}{(N/2)\cdot sumw_c}\sum_{n=1}^{N/2}\left(\frac{\mathrm{Im}\left(\sum_{i=1}^{L}u_{i,n}\cdot H_{i,n}^{*}\cdot S_n^{*}\right)}{\mathrm{Re}\left(\sum_{i=1}^{L}u_{i,n}\cdot H_{i,n}^{*}\cdot S_n^{*}\right)}+\frac{\mathrm{Im}\left(\sum_{i=1}^{L}u_{i,-n}\cdot H_{i,-n}^{*}\cdot S_{-n}^{*}\right)}{\mathrm{Re}\left(\sum_{i=1}^{L}u_{i,-n}\cdot H_{i,-n}^{*}\cdot S_{-n}^{*}\right)}\right)\cdot\min\left(\sum_{i=1}^{L}\left|H_{i,n}\right|^2,\sum_{i=1}^{L}\left|H_{i,-n}\right|^2\right) \quad (58)$$

$$\Delta\phi_s = \frac{1}{(N/2+1)(N/2)\cdot sumw_s}\sum_{n=1}^{N/2}\left(\frac{\mathrm{Im}\left(\sum_{i=1}^{L}u_{i,n}\cdot H_{i,n}^{*}\cdot S_n^{*}\right)}{\mathrm{Re}\left(\sum_{i=1}^{L}u_{i,n}\cdot H_{i,n}^{*}\cdot S_n^{*}\right)}-\frac{\mathrm{Im}\left(\sum_{i=1}^{L}u_{i,n-N/2-1}\cdot H_{i,n-N/2-1}^{*}\cdot S_{n-N/2-1}^{*}\right)}{\mathrm{Re}\left(\sum_{i=1}^{L}u_{i,n-N/2-1}\cdot H_{i,n-N/2-1}^{*}\cdot S_{n-N/2-1}^{*}\right)}\right)\cdot\min\left(\sum_{i=1}^{L}\left|H_{i,n}\right|^2,\sum_{i=1}^{L}\left|H_{i,n-N/2-1}\right|^2\right) \quad (59)$$

where $sumw_c = \sum_{n=1}^{N/2}\min\left(\sum_{i=1}^{L}\left|H_{i,n}\right|^2,\sum_{i=1}^{L}\left|H_{i,-n}\right|^2\right)$ and

$sumw_s = \sum_{n=1}^{N/2}\min\left(\sum_{i=1}^{L}\left|H_{i,n}\right|^2,\sum_{i=1}^{L}\left|H_{i,n-N/2-1}\right|^2\right)$.

[0082] FIG. 19 is a block diagram illustrating an example implementation of a phase error estimator 74'' for performing calculations as indicated in expressions (60) and (61) above. Phase error estimator 74'' conforms almost identically to phase error

estimator 74' of FIG. 18. Instead of extracting the real and imaginary components of the input signal, however, phase error estimator 74'' extracts only the imaginary component (106). Again, the phase error is small under normal operating conditions. As a result, the imaginary part of $\sum_{i=1}^{L} u_{i,n} \cdot H_{i,n}^{*} \cdot S_{n}^{*}$ is much smaller than the real part, so a phase error estimate proportional to the actual phase error can be obtained using phase error estimator 74'' according to the expressions:

$$\Delta\phi_c = \frac{1}{(N/2)\cdot sumw_c}\sum_{n=1}^{N/2}\left(\mathrm{Im}\left(\sum_{i=1}^{L} u_{i,n}\cdot H_{i,n}^{*}\cdot S_{n}^{*}\right)+\mathrm{Im}\left(\sum_{i=1}^{L} u_{i,-n}\cdot H_{i,-n}^{*}\cdot S_{-n}^{*}\right)\right)\cdot \min\left(\sum_{i=1}^{L}\left|H_{i,n}\right|^2,\sum_{i=1}^{L}\left|H_{i,-n}\right|^2\right) \quad (60)$$

$$\Delta\phi_s = \frac{1}{(N/2+1)(N/2)\cdot sumw_s}\sum_{n=1}^{N/2}\left(\mathrm{Im}\left(\sum_{i=1}^{L} u_{i,n}\cdot H_{i,n}^{*}\cdot S_{n}^{*}\right)-\mathrm{Im}\left(\sum_{i=1}^{L} u_{i,n-N/2-1}\cdot H_{i,n-N/2-1}^{*}\cdot S_{n-N/2-1}^{*}\right)\right)\cdot \min\left(\sum_{i=1}^{L}\left|H_{i,n}\right|^2,\sum_{i=1}^{L}\left|H_{i,n-N/2-1}\right|^2\right) \quad (61)$$

[0083] FIG. 20 is a block diagram illustrating an example implementation of a phase error estimator 74''' for performing calculations as indicated in expressions (62) and (63) above. Phase error estimator 74''' conforms almost identically to phase error estimator 74 of FIG. 17. Instead of extracting the real and imaginary components of the input signal, however, phase error estimator 74''' extracts only the imaginary component (108). The implementation shown in FIG. 20 enables calculations of phase error estimates according to the following expressions:

$$\Delta\phi_c = \frac{1}{(N/2)}\sum_{n=1}^{N/2}\left(\mathrm{Im}\left(\sum_{i=1}^{L} u_{i,n}\cdot H_{i,n}^{*}\cdot S_{n}^{*}\right)+\mathrm{Im}\left(\sum_{i=1}^{L} u_{i,-n}\cdot H_{i,-n}^{*}\cdot S_{-n}^{*}\right)\right) \quad (62)$$

$$\Delta\phi_s = \frac{1}{(N/2+1)(N/2)}\sum_{n=1}^{N/2}\left(\mathrm{Im}\left(\sum_{i=1}^{L} u_{i,n}\cdot H_{i,n}^{*}\cdot S_{n}^{*}\right)-\mathrm{Im}\left(\sum_{i=1}^{L} u_{i,n-N/2-1}\cdot H_{i,n-N/2-1}^{*}\cdot S_{n-N/2-1}^{*}\right)\right) \quad (63)$$

[0084] FIG. 21 is a flow diagram illustrating joint performance of equalization, soft-demapping and phase error estimation functions. The method illustrated in FIG. 21 may make use of various hardware and functional embodiments described herein. As shown in FIG. 21, a method for equalization, soft-demapping and phase error estimation involves receiving wireless signals via multiple antennas (110), sampling the signals with an analog-to-digital converter according to an FFT sampling window

(112), and demodulating the sampled wireless signals to produce observations of quadrature amplitude modulation (QAM) symbols (114).

[0085] Upon estimating the channel responses for the signal paths associated with the antennas (116), the method involves equalizing each of the QAM symbol observations based on estimated channel responses (118). The QAM symbol observations are corrected for phase error (120), preferably including both carrier phase error and sampling phase error. The method then involves combining the QAM symbol observations (122), followed by application of a soft decision function (124) to carry out generation of soft decision bits (128), i.e., performance of the soft demapping function. Using the soft decision bits, the method further involves estimating phase error (128). This estimate can be used to make sampling phase error and carrier phase error adjustments, i.e., corrections, for subsequent observation samples. Then, branch metrics for the convolutional decoder are calculated using the soft decision bits (130), and the process repeats for subsequent samples.

[0086] The various components described herein for joint equalization, soft demapping and phase error estimation may be formed by a variety of hardware such as integrated logic circuitry, e.g., an Application Specific Integrated Circuit (ASIC), programmable logic devices, microprocessors, and the like. For size and complexity reasons, it is desirable that the various equalizations, soft demapping and phase error estimation circuitry be formed together within a common hardware device such as an ASIC.

CLAIMS:

1. A method comprising:

receiving wireless signals via multiple antennas;

demodulating the wireless signals to produce observations of a transmitted symbol;

weighting each of the observations with a complex-conjugate of a channel response for the corresponding antenna;

combining the weighted observations to form a combined observation; and

generating one or more soft decision bits indicative of the transmitted symbol for the combined observation according to soft demapping rules based on a subset of the transmitted symbol constellation.

2. The method of claim 1, wherein the soft demapping rules are based on a first minimum distance symbol associated with bit 1 and a second minimum distance symbol associated with bit 0, and wherein the minimum distance symbols are constrained to be within a predetermined distance of an inter-bit decision boundary.

3. The method of claim 1, wherein the soft demapping rules are based on piecewise linear functions of real and imaginary components of the combined observation and a combined energy of the channel responses for the multiple antennas, the method further comprising computing one or more of the soft decisions recursively based on previously computed soft decisions.

4. The method of any of claims 1 to 3, wherein the wireless signals are multi-carrier (MC) signals, the method further comprising applying a Fourier transform function to obtain the observations of the transmitted symbol.

5. The method of claim 1, further comprising estimating a combined phase error including carrier phase error and sampling phase error for the combined observation using one of the transmitted symbol estimated based on the soft decision bits and a predetermined symbol transmitted via a pilot tone, and performing the generation and estimation functions jointly within shared hardware.

6. A method comprising:

receiving orthogonal frequency division multiplexing (OFDM) wireless signals via multiple antennas;

demodulating and performing fast Fourier transform (FFT) functions on the wireless signals to produce observations of a transmitted quadrature amplitude modulated (QAM) symbol;

weighting each of the observations with a complex-conjugate of a channel response for the corresponding antenna;

combining the weighted observations to form a combined observation; and

generating one or more soft decision bits indicative of the transmitted QAM symbol for the combined observation according to soft demapping rules based on a subset of the transmitted QAM symbol constellation.

7. The method of claim 6, wherein the soft demapping rules are based on a first minimum distance symbol associated with bit 1 and a first minimum distance symbol associated with bit 0, wherein the minimum distance symbols are constrained to be within a predetermined distance of an inter-bit decision boundary.

8. The method of claim 6, wherein the soft demapping rules are based on piecewise linear functions of real and imaginary components of the combined observation and a combined energy of the channel responses for the multiple antennas, the method further comprising computing one or more of the soft decisions recursively based on previously computed soft decisions.

9. The method of any of claims 6 to 8, further comprising estimating a combined phase error including carrier phase error and sampling phase error for the combined observation using one of the transmitted symbol estimated based on the soft decision bits and a predetermined symbol transmitted via a pilot tone.

10. The method of claim 6, further comprising:

estimating a combined phase error including carrier phase error and sampling phase error for the combined observation using one of the transmitted symbol estimated based on the soft decision bits and a predetermined symbol transmitted via a pilot tone;

estimating the carrier phase error by summing the estimated combined phase errors that correspond to complementary subcarriers in the wireless signals to remove the sampling phase error; and

estimating the sampling phase error by subtracting the estimated combined phase error that corresponds to one of the subcarriers from the estimated combined phase error that corresponds to another of the subcarriers.

11. The method of claim 10, further comprising:

adjusting an FFT sampling window for each of the wireless signals based on the sampling phase error; and

applying a frequency domain correction to subsequent observations based on the carrier phase error and sampling phase error.

12. The method of claim 10, further comprising applying a time domain correction to subsequent observations based on the carrier phase error and sampling phase error.

13. The method of claim 10, further comprising:

adjusting an FFT sampling window for each of the wireless signals based on the sampling phase error;

applying a time domain correction to subsequent observations based on the carrier phase error; and

applying a frequency domain correction to subsequent observations based on the sampling phase error.

14. The method of claim 10, further comprising performing the generation and estimation functions jointly within shared hardware.

15. A method comprising:

receiving an orthogonal frequency division multiplexing (OFDM) wireless signal via a first antenna;

receiving the orthogonal frequency division multiplexing (OFDM) wireless signal via a second antenna;

demodulating and performing fast Fourier transform (FFT) functions on the wireless signal received by the first antenna to produce a first observation of a transmitted quadrature amplitude modulated (QAM) symbol;

demodulating and performing fast Fourier transform (FFT) functions on the wireless signal received by the second antenna to produce a second observation of the transmitted quadrature amplitude modulated (QAM) symbol;

weighting the first observation with a complex-conjugate of a channel response for the first antenna;

weighting the second observation with a complex-conjugate of a channel response for the second antenna;

combining the weighted first observation and the weighted second observation to form a combined observation; and

generating one or more soft decision bits indicative of the transmitted QAM symbol for the combined observation according to soft demapping rules based on a subset of the transmitted QAM symbol constellation.

16. The method of claim 15, wherein the soft demapping rules are based on a first minimum distance symbol associated with bit 1 and a first minimum distance symbol associated with bit 0, wherein the minimum distance symbols are constrained to be within a predetermined distance of an inter-bit decision boundary.

17. The method of claim 15, wherein the soft demapping rules are based on piecewise linear functions of real and imaginary components of the combined observation and a combined energy of the channel responses for the multiple antennas, the method further comprising computing one or more of the soft decisions recursively based on previously computed soft decisions.

18. A method comprising:

receiving an orthogonal frequency division multiplexing (OFDM) wireless signal via an antenna;

demodulating and performing a fast Fourier transform (FFT) function on the wireless signal to produce an observation of a transmitted quadrature amplitude modulated (QAM) symbol;

weighting the observation with a complex-conjugate of a channel response for the antenna; and

generating one or more soft decision bits indicative of the transmitted symbol for the weighted observation according to soft demapping rules based on a subset of the transmitted symbol constellation.

19. The method of claim 18, wherein the soft demapping rules are based on a first minimum distance symbol associated with bit 1 and a second minimum distance symbol associated with bit 0, wherein the minimum distance symbols are constrained to be within a predetermined distance of an inter-bit decision boundary.

20. The method of claim 18, wherein the soft demapping rules are based on piecewise linear functions of real and imaginary components of the weighted observation and the energy of the channel response, the method further comprising computing one or more of the soft decisions recursively based on previously computed soft decisions.

21. The method of any of claims 18 to 20, further comprising:

estimating a combined phase error including carrier phase error and sampling phase error for the weighted observation using one of the transmitted symbol estimated based on the soft decision bits or a predetermined symbol transmitted via a pilot tone;

estimating the carrier phase error by summing the estimated combined phase errors that correspond to complementary subcarriers in the wireless signals to remove the sampling phase error; and

estimating the sampling phase error by subtracting the estimated combined phase error that corresponds to one of the subcarriers from the estimated combined phase error that corresponds to another of the subcarriers.

22. The method of claim 21, further comprising:

estimating a combined phase error including carrier phase error and sampling phase error for the weighted observation using one of the transmitted symbol estimated based on the soft decision bits or a predetermined symbol transmitted via a pilot tone;

estimating the carrier phase error by summing the estimated combined phase errors that correspond to complementary subcarriers in the wireless signals to remove the sampling phase error;

estimating the sampling phase error by subtracting the estimated combined phase error that corresponds to one of the subcarriers from the estimated combined phase error that corresponds to another of the subcarriers;

adjusting an FFT sampling window for the wireless signal based on the sampling phase error; and

applying a frequency domain correction to subsequent observations based on the carrier phase error and sampling phase error.

23. The method of claim 22, further comprising:

adjusting an FFT sampling window for the wireless signal based on the sampling phase error;

applying a time domain correction to subsequent observations based on the carrier phase error; and

applying a frequency domain correction to subsequent observations based on the sampling phase error.

24. The method of claim 21, further comprising performing the generation and estimation functions jointly within shared hardware.

25. A wireless receiver configured to perform the method of any of claims 1 through 24, the receiver comprising:

multiple antennas that receive wireless signals;

a demodulator that demodulates the wireless signals to produce observations of a transmitted symbol;

an equalizer that weights each of the observations with a complex conjugate of an estimated channel response for the corresponding antenna; and

a soft demapper unit that combines the weighted observations to form a combined observation, and generates one or more soft decision bits indicative of the transmitted symbol for the combined observation according to soft demapping rules based on a subset of the transmitted symbol constellation.

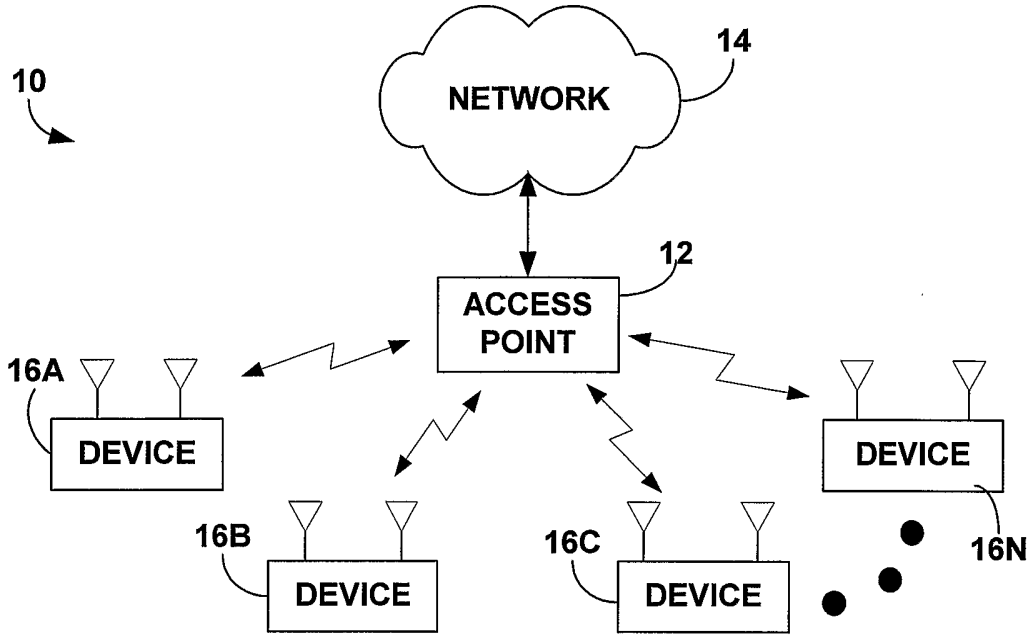

10
NETWORK
14
12
ACCESS POINT
16A
DEVICE
DEVICE
16N
16B
DEVICE
16C
DEVICE

FIG. 1

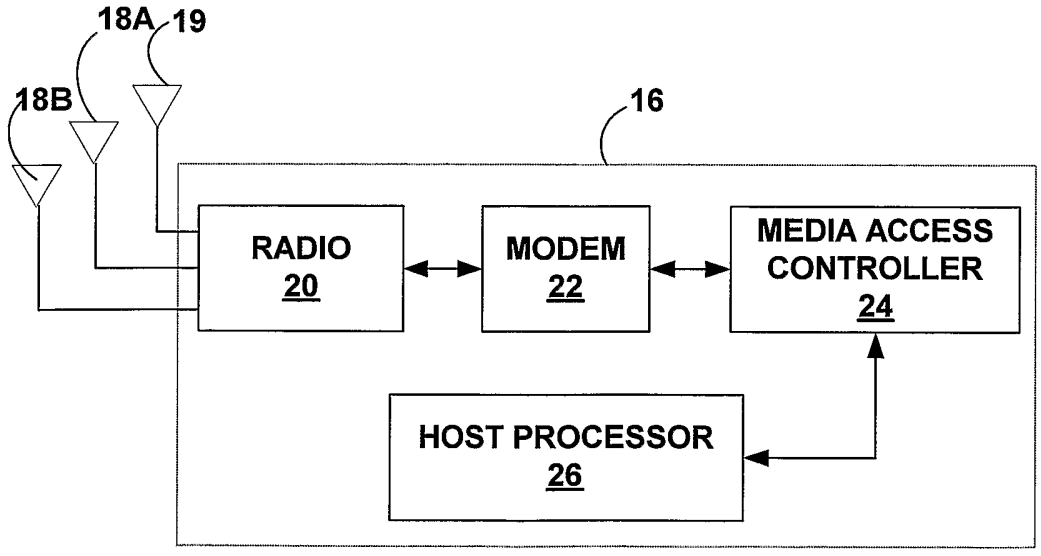

18A
19
18B
16
RADIO 20
MODEM 22
MEDIA ACCESS CONTROLLER 24
HOST PROCESSOR 26

FIG. 2

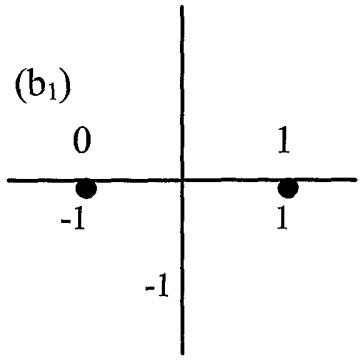


FIG. 3

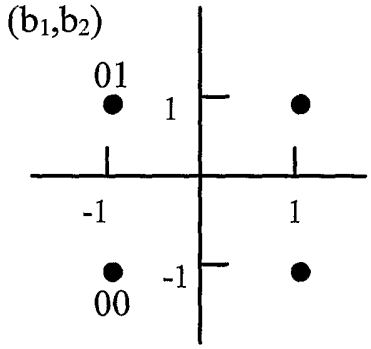


FIG. 4

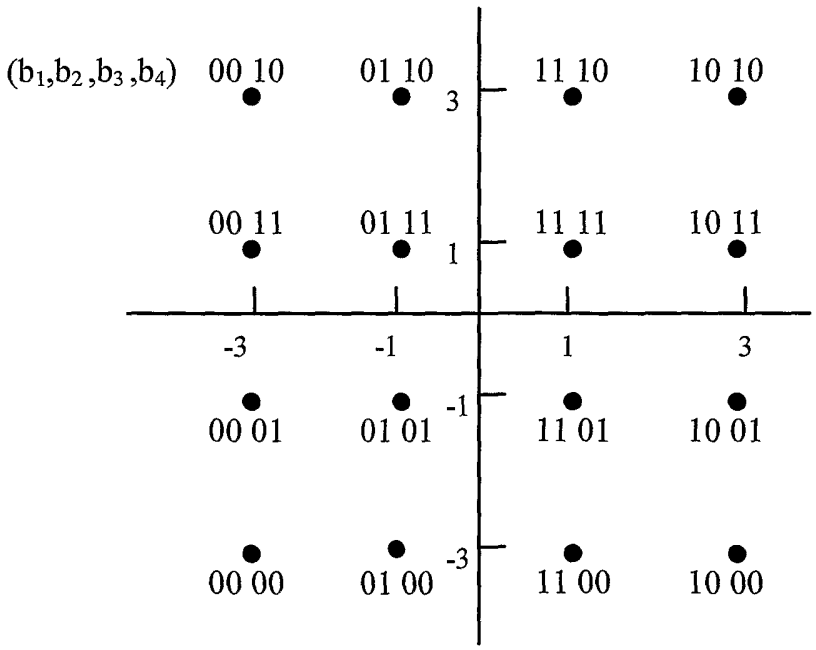
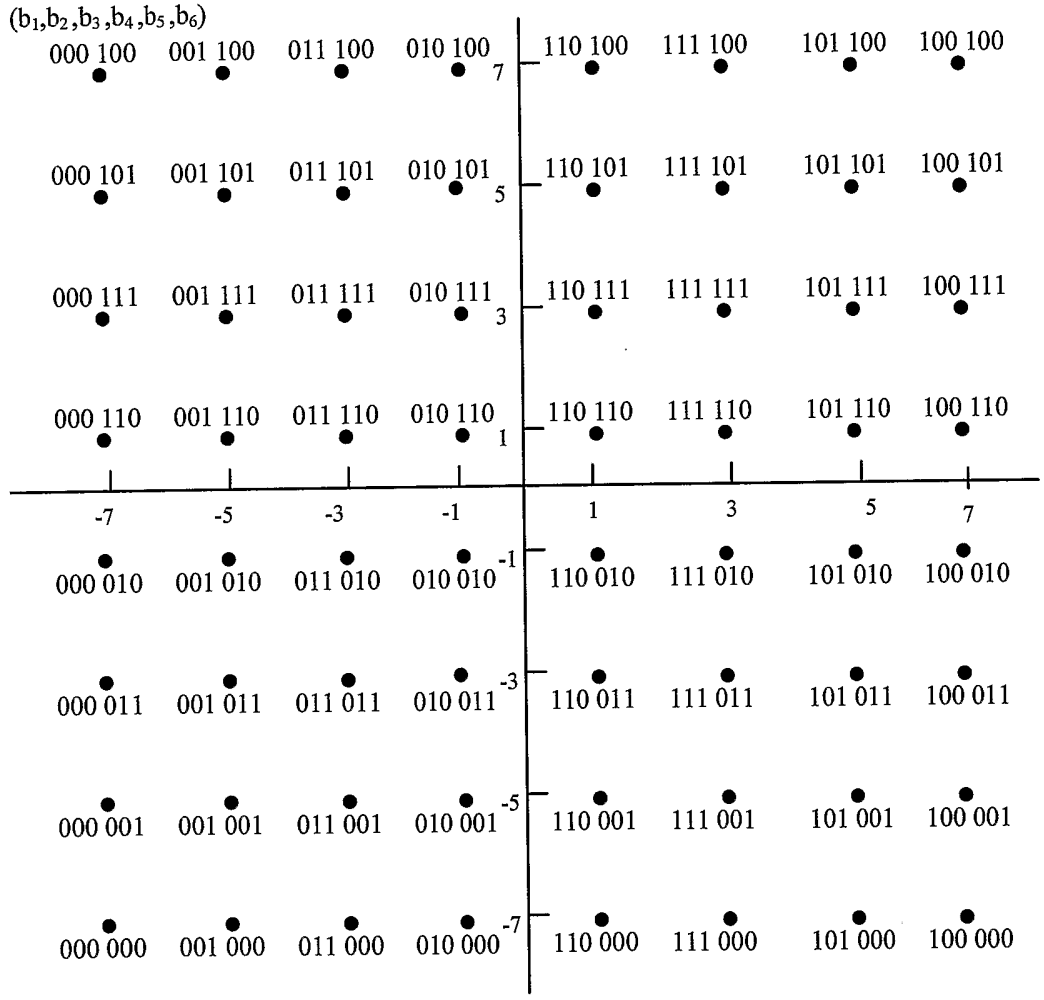


FIG. 5


(b1,b2,b3,b4,b5,b6)
000 100 001 100 011 100 010 100 110 100 111 100 101 100 100 100
000 101 001 101 011 101 010 101 110 101 111 101 101 101 100 101
000 111 001 111 011 111 010 111 110 111 111 111 101 111 100 111
000 110 001 110 011 110 010 110 110 110 111 110 101 110 100 110
7
5
3
1
-7 -5 -3 -1 1 3 5 7
000 010 001 010 011 010 010 110 010 111 010 101 010 100 010
000 011 001 011 011 011 010 011 110 011 111 011 101 011 100 011
000 001 001 001 011 001 010 001 110 001 111 001 101 001 100 001
000 000 001 000 011 000 010 000 110 000 111 000 101 000 100 000
-1
-3
-5
-7

64-QAM

FIG. 6

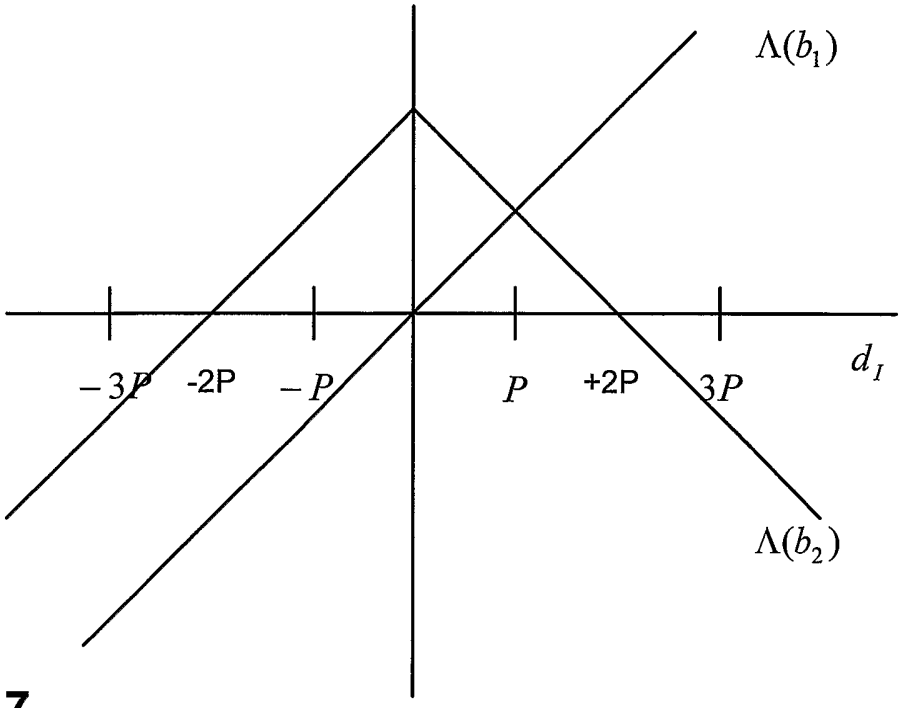

$\Lambda(b_1)$
d_I
$-3P$
-2P
$-P$
P
+2P
$3P$
$\Lambda(b_2)$

FIG. 7

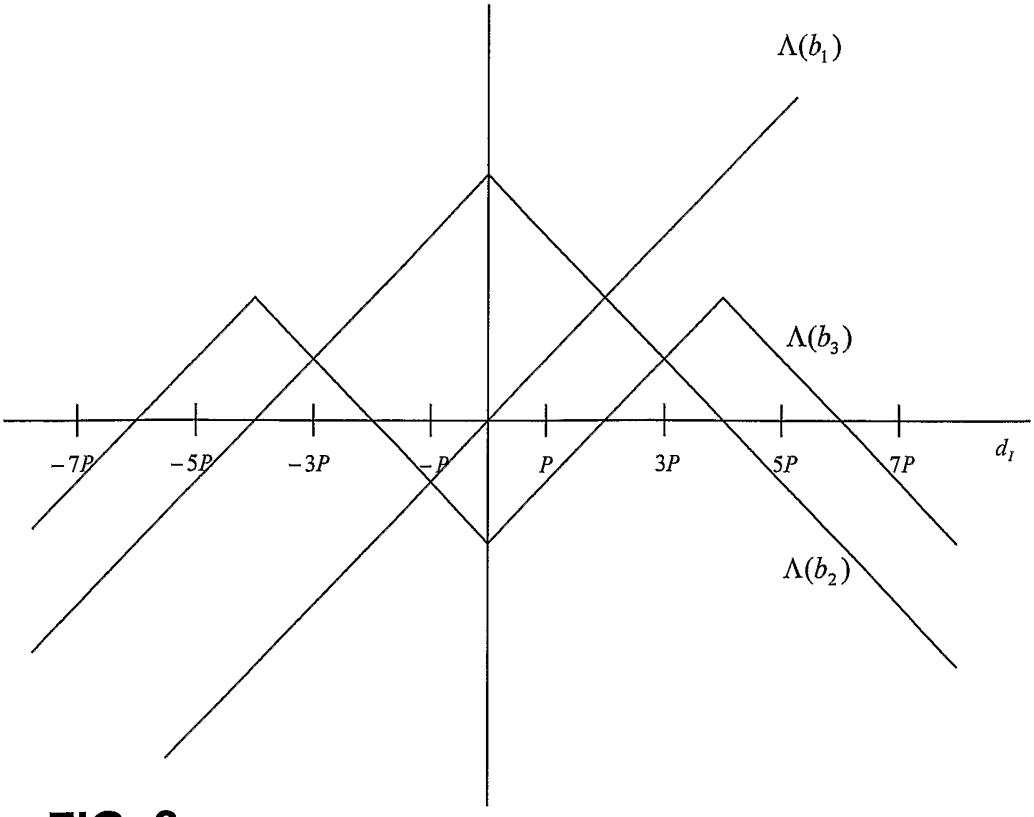

$\Lambda(b_1)$
$\Lambda(b_3)$
d_I
$-7P$
$-5P$
$-3P$
$-P$
P
$3P$
$5P$
$7P$
$\Lambda(b_2)$

FIG. 8

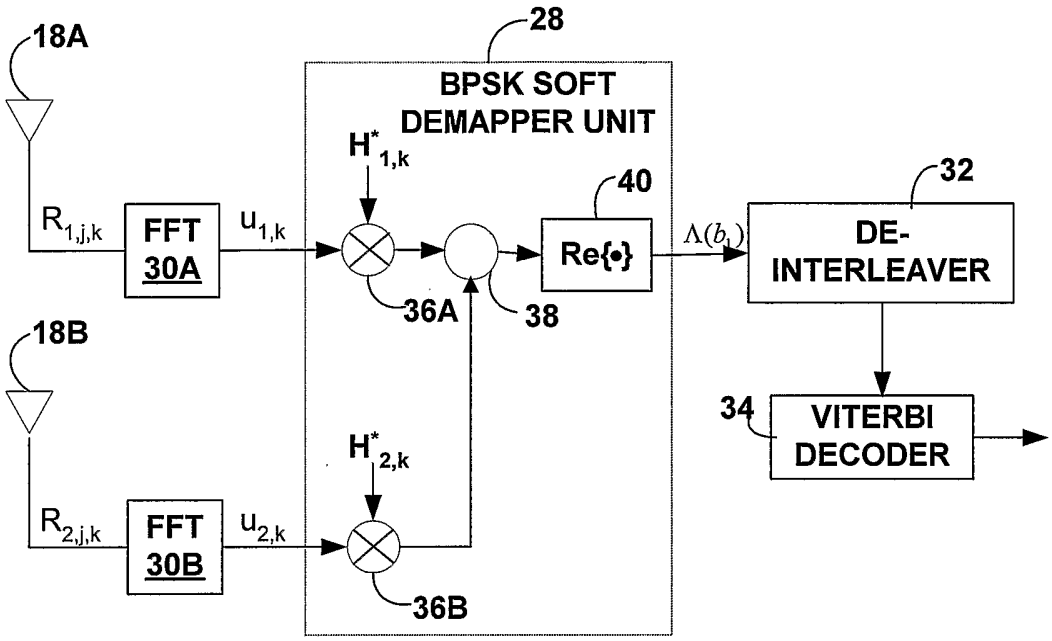

18A
28
BPSK SOFT
DEMAPPER UNIT
$H^*_{1,k}$
40
32
$R_{1,j,k}$
FFT
30A
$u_{1,k}$
Re{•}
$\Lambda(b_1)$
DE-
INTERLEAVER
36A
38
18B
34
VITERBI
DECODER
$H^*_{2,k}$
$R_{2,j,k}$
FFT
30B
$u_{2,k}$
36B

FIG. 9

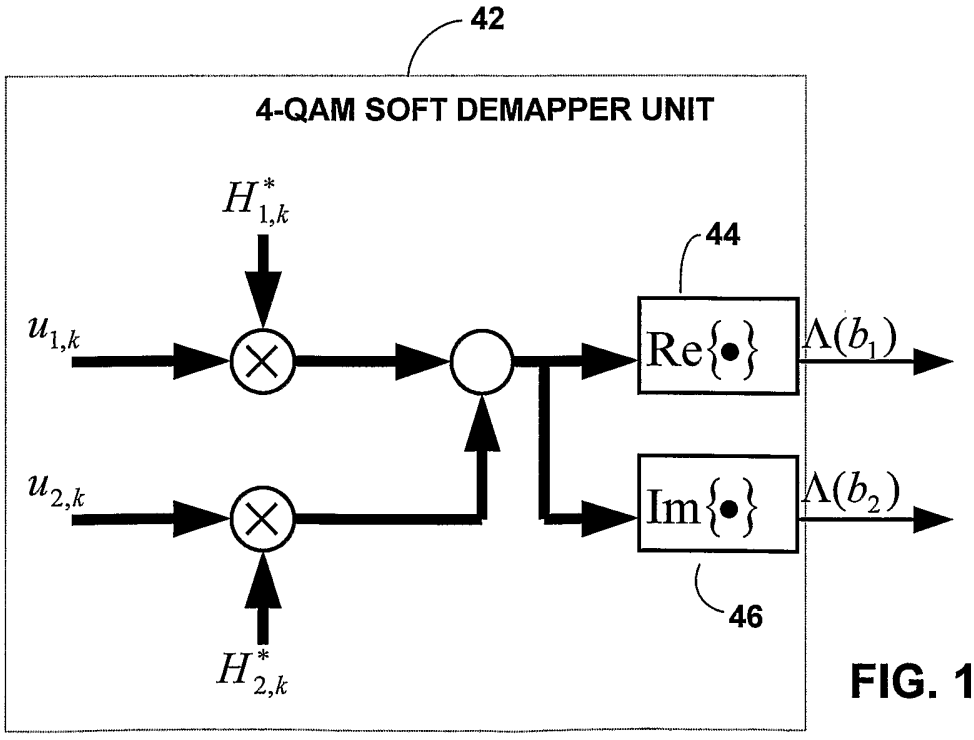

42
4-QAM SOFT DEMAPPER UNIT
$H^*_{1,k}$
44
$u_{1,k}$
Re{•}
$\Lambda(b_1)$
$u_{2,k}$
Im{•}
$\Lambda(b_2)$
46
$H^*_{2,k}$

FIG. 10

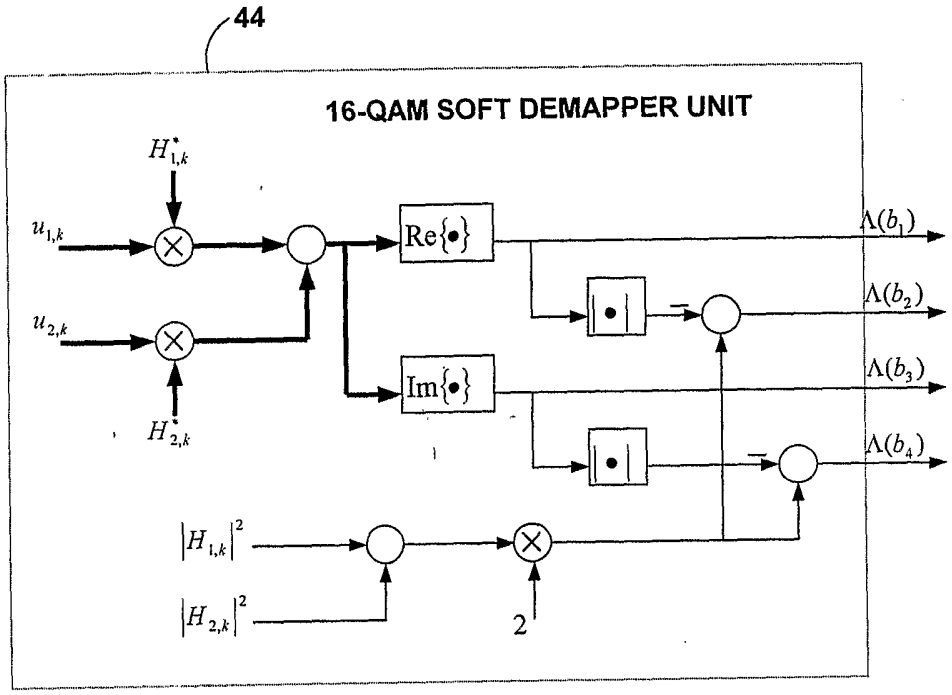

44
16-QAM SOFT DEMAPPER UNIT
$H^*_{1,k}$
$u_{1,k}$
$u_{2,k}$
$H^*_{2,k}$
Re{•}
Im{•}
|•|
$\Lambda(b_1)$
$\Lambda(b_2)$
$\Lambda(b_3)$
$\Lambda(b_4)$
$|H_{1,k}|^2$
$|H_{2,k}|^2$
2

FIG. 11

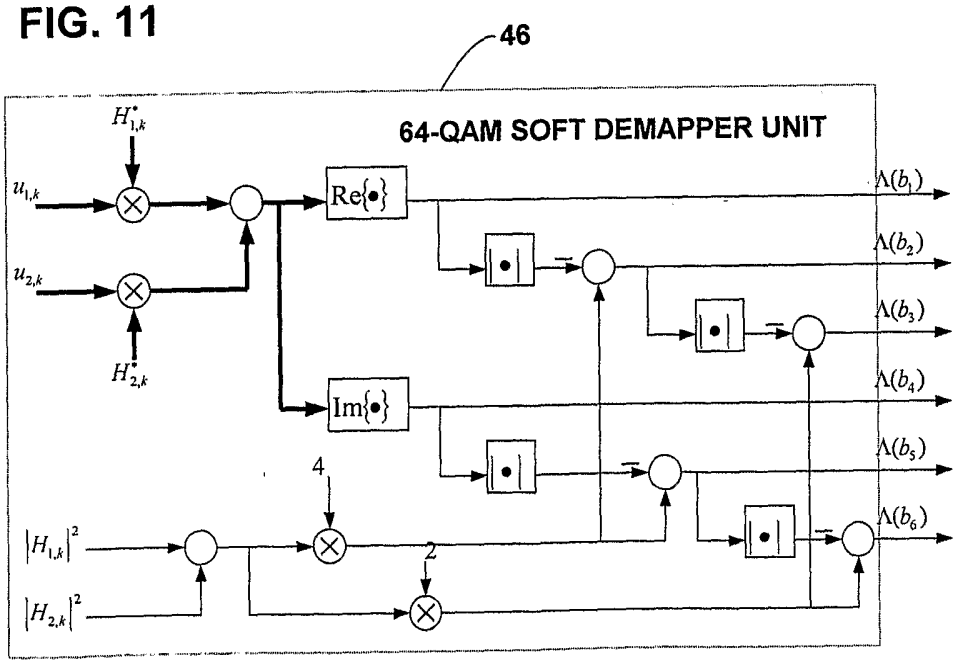

46
64-QAM SOFT DEMAPPER UNIT
$H^*_{1,k}$
$u_{1,k}$
$u_{2,k}$
$H^*_{2,k}$
Re{•}
Im{•}
|•|
$\Lambda(b_1)$
$\Lambda(b_2)$
$\Lambda(b_3)$
$\Lambda(b_4)$
$\Lambda(b_5)$
$\Lambda(b_6)$
4
2
$|H_{1,k}|^2$
$|H_{2,k}|^2$

FIG. 12

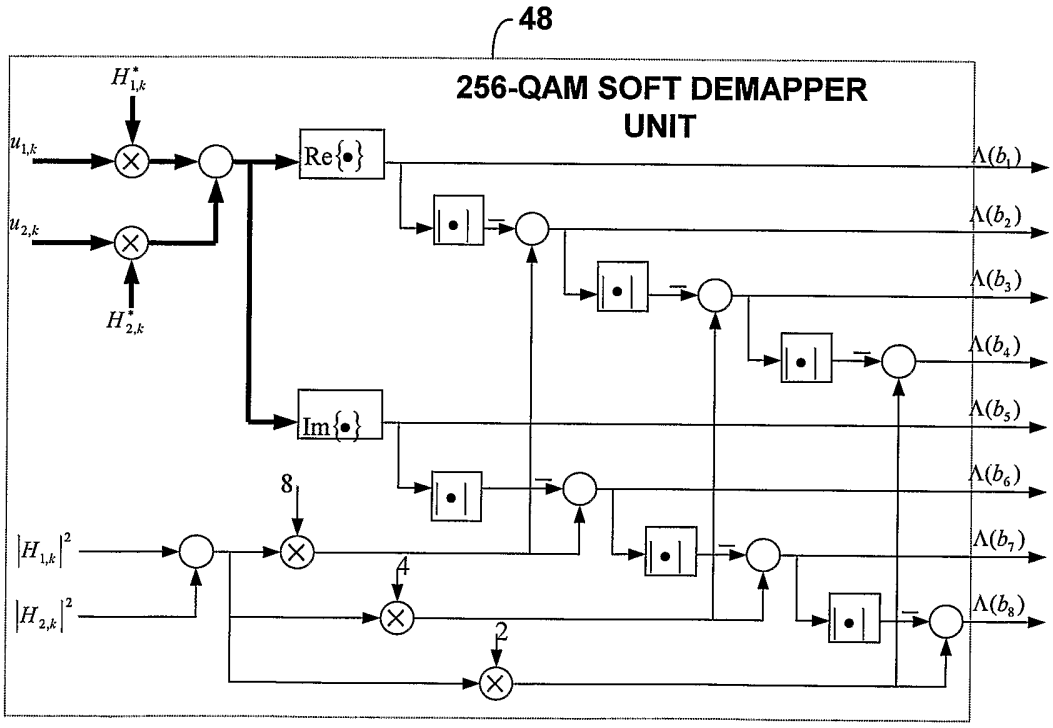

48
256-QAM SOFT DEMAPPER UNIT
$H^*_{1,k}$
$u_{1,k}$
$u_{2,k}$
$H^*_{2,k}$
Re{•}
Im{•}
|•|
8
4
2
$|H_{1,k}|^2$
$|H_{2,k}|^2$
$\Lambda(b_1)$
$\Lambda(b_2)$
$\Lambda(b_3)$
$\Lambda(b_4)$
$\Lambda(b_5)$
$\Lambda(b_6)$
$\Lambda(b_7)$
$\Lambda(b_8)$

FIG. 13

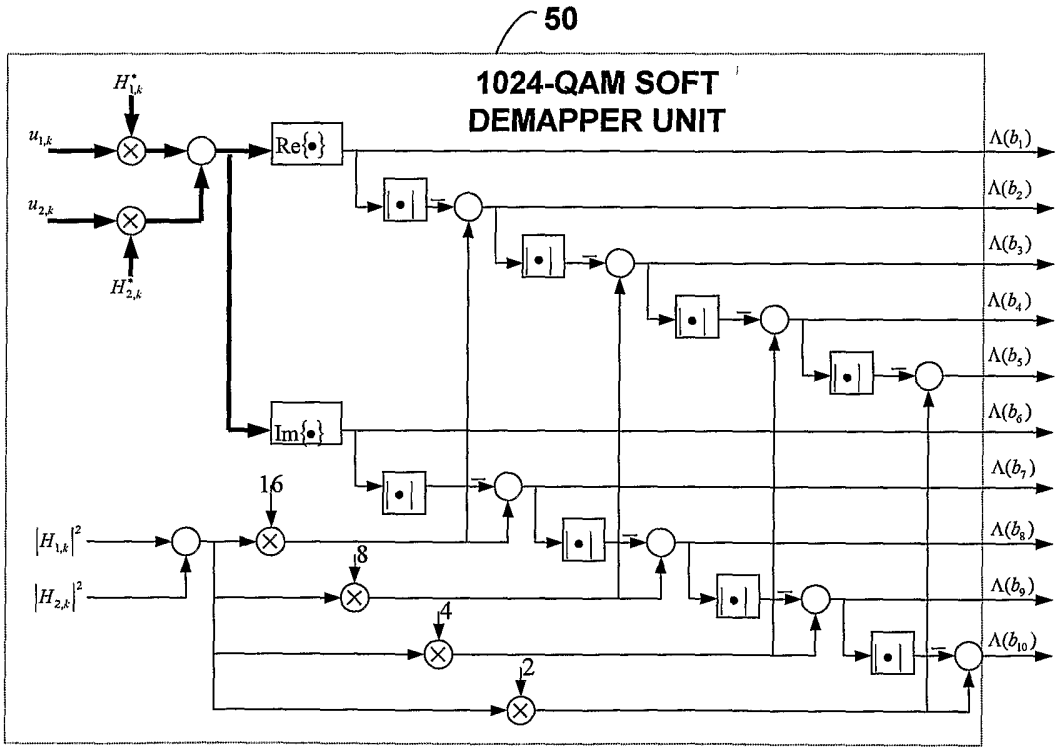

50
1024-QAM SOFT
DEMAPPER UNIT
$H^*_{1,k}$
$u_{1,k}$
$u_{2,k}$
$H^*_{2,k}$
Re{•}
Im{•}
16
8
4
2
$|H_{1,k}|^2$
$|H_{2,k}|^2$
$\Lambda(b_1)$
$\Lambda(b_2)$
$\Lambda(b_3)$
$\Lambda(b_4)$
$\Lambda(b_5)$
$\Lambda(b_6)$
$\Lambda(b_7)$
$\Lambda(b_8)$
$\Lambda(b_9)$
$\Lambda(b_{10})$

FIG. 14

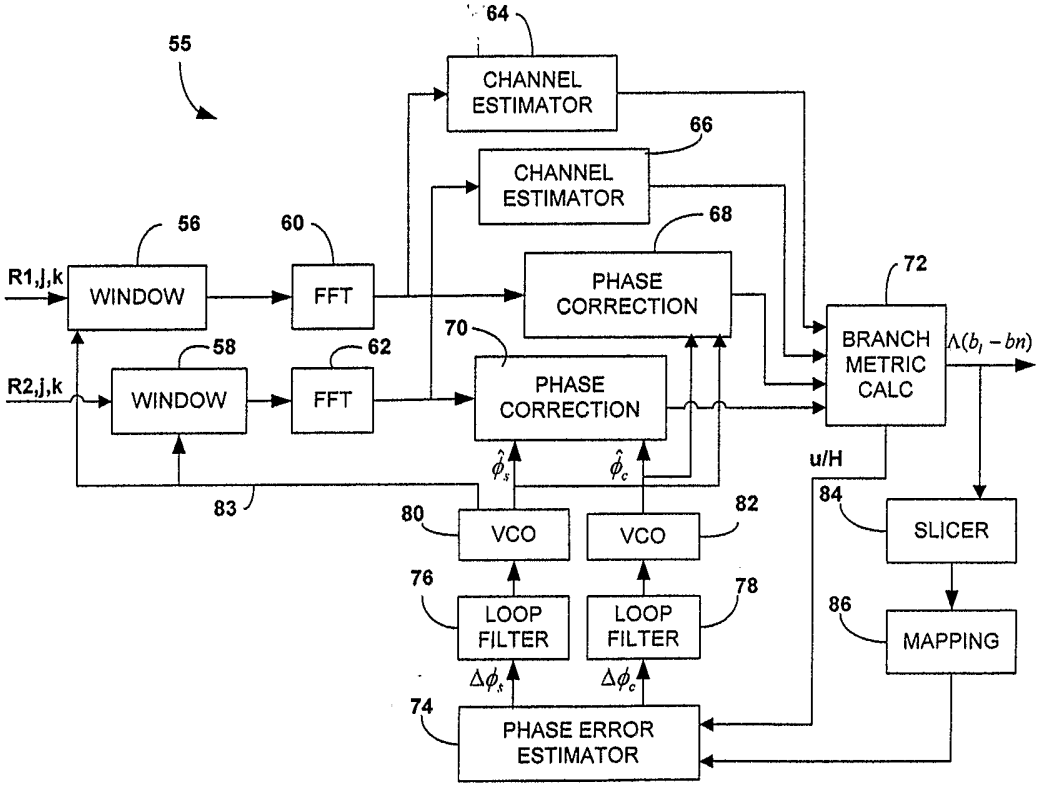

55
64
CHANNEL ESTIMATOR
66
CHANNEL ESTIMATOR
68
PHASE CORRECTION
72
BRANCH METRIC CALC
$\Lambda(b_l - bn)$
56
60
R1,j,k
WINDOW
FFT
58
62
70
R2,j,k
WINDOW
FFT
PHASE CORRECTION
$\hat{\phi}_s$
$\hat{\phi}_c$
u/H
83
80
VCO
VCO
82
84
SLICER
76
LOOP FILTER
LOOP FILTER
78
86
MAPPING
$\Delta\phi_s$
$\Delta\phi_c$
74
PHASE ERROR ESTIMATOR

FIG. 15

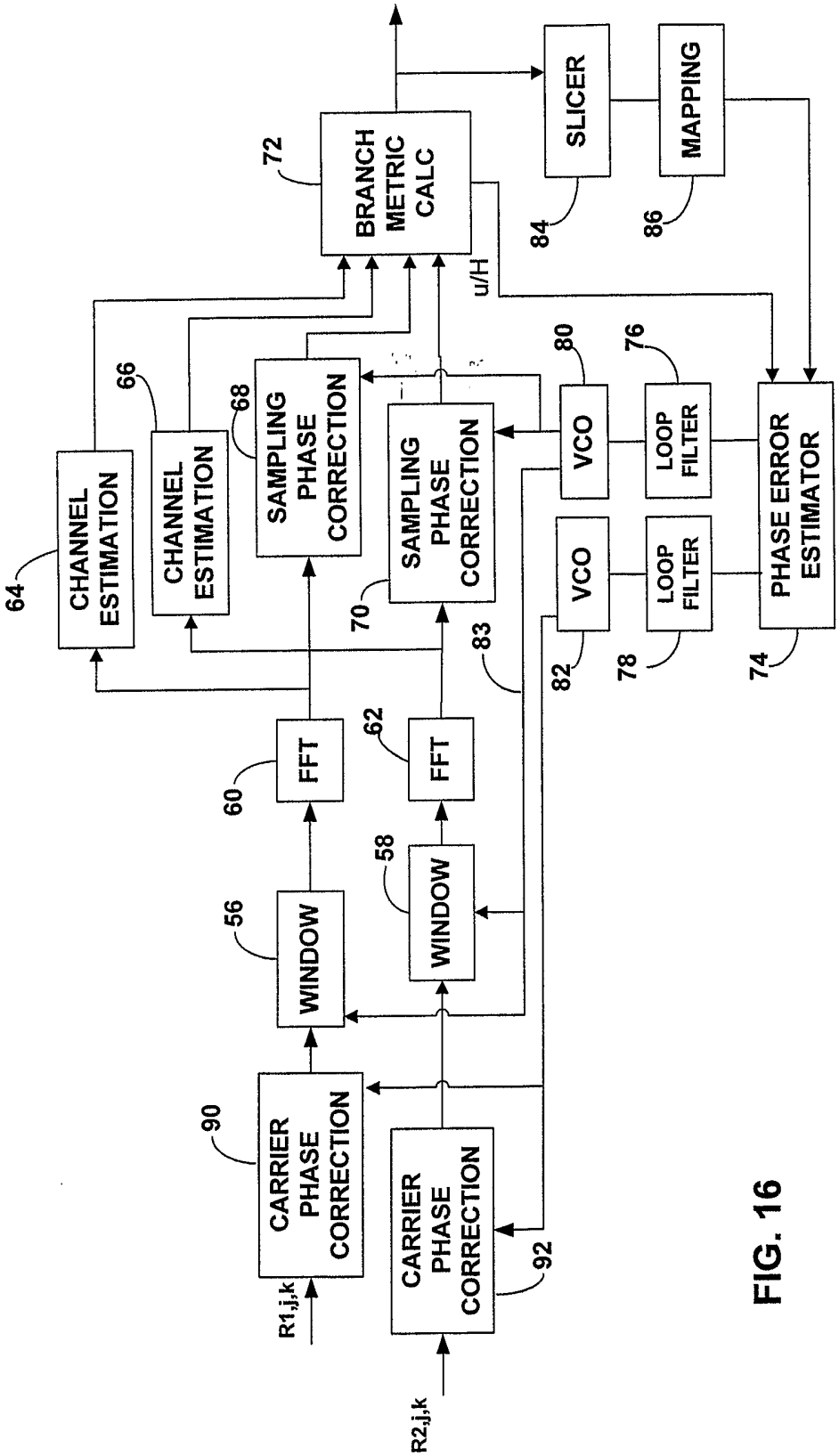

SLICER
MAPPING
BRANCH METRIC CALC
72
84
86
u/H
80
76
66
68
SAMPLING PHASE CORRECTION
VCO
LOOP FILTER
CHANNEL ESTIMATION
CHANNEL ESTIMATION
SAMPLING PHASE CORRECTION
PHASE ERROR ESTIMATOR
64
70
83
82
78
74
FFT
FFT
60
62
58
WINDOW
WINDOW
56
90
CARRIER PHASE CORRECTION
CARRIER PHASE CORRECTION
92
R1j,j,k
R2j,j,k

FIG. 16

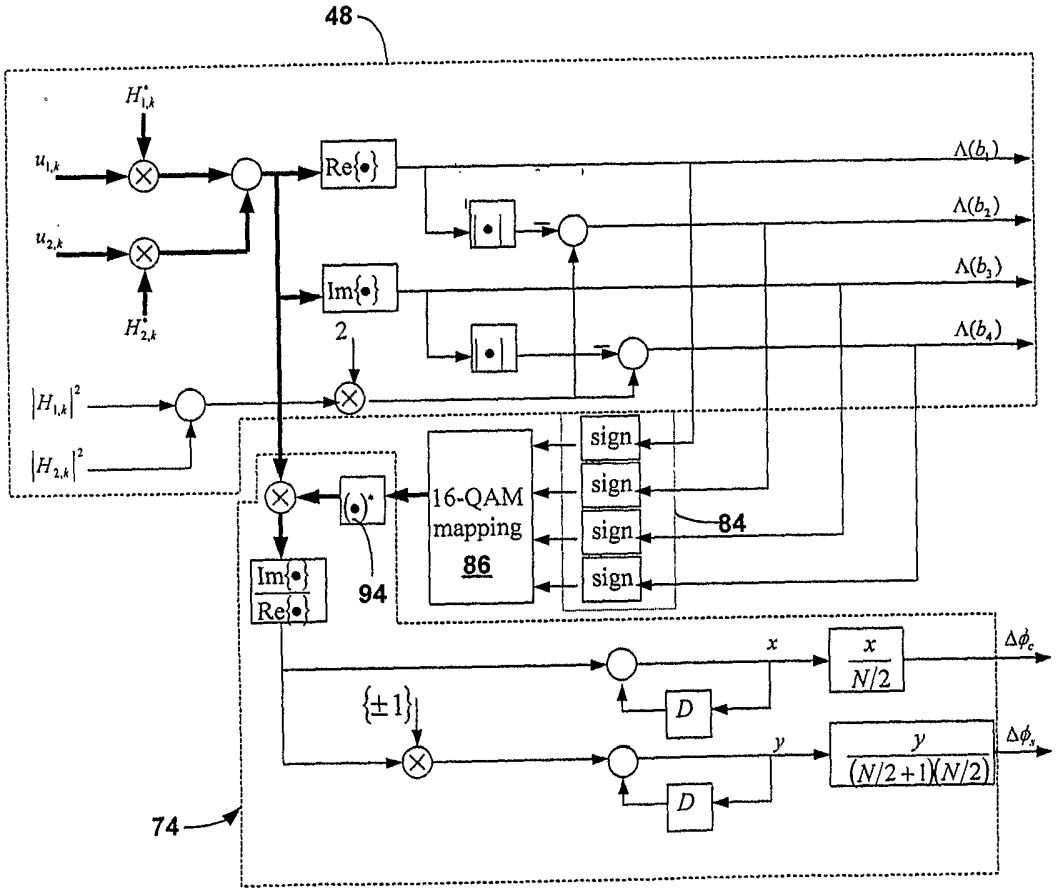

48
$H_{1,k}^*$
$u_{1,k}$
$u_{2,k}$
$H_{2,k}^*$
Re{•}
Im{•}
2
$|H_{1,k}|^2$
$|H_{2,k}|^2$
$\Lambda(b_1)$
$\Lambda(b_2)$
$\Lambda(b_3)$
$\Lambda(b_4)$
sign
sign
sign
sign
84
16-QAM mapping
86
(•)*
94
Im{•}
Re{•}
{±1}
D
D
x
y
$\frac{x}{N/2}$
$\frac{y}{(N/2+1)(N/2)}$
$\Delta\phi_x$
$\Delta\phi_y$
74

FIG. 17

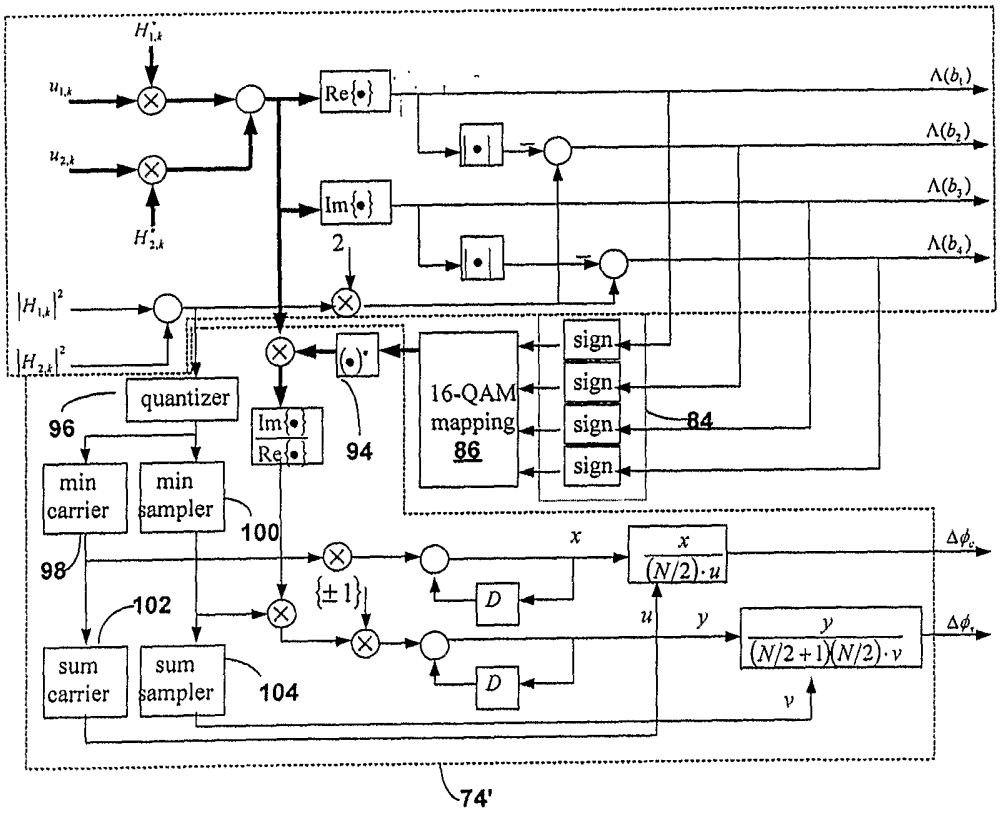

Re{•}
Im{•}
2
quantizer
96
min carrier
min sampler
100
98
102
sum carrier
sum sampler
104
16-QAM mapping 86
84
sign
sign
sign
sign
94
{±1}
D
D
x
u
y
v
74'

FIG. 18

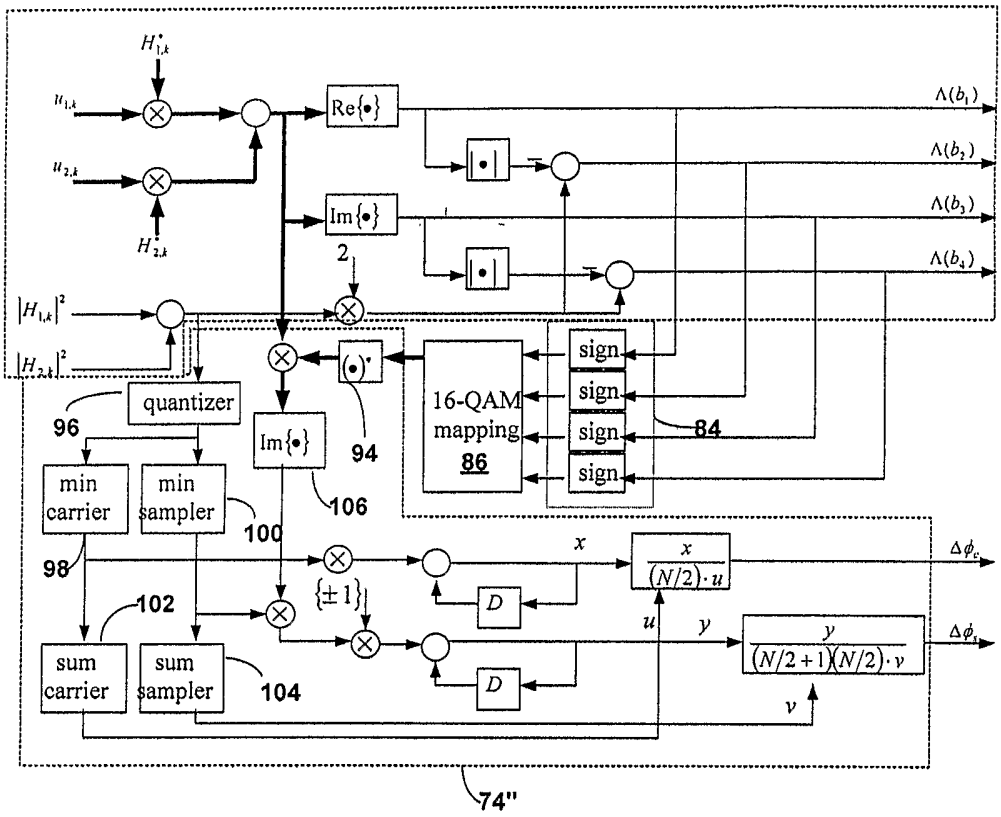

Re{•}
Im{•}
2
16-QAM mapping 86
sign
sign
sign
sign
84
quantizer
96
min carrier
min sampler
100
98
102
sum carrier
sum sampler
104
Im{•}
94
106
{±1}
D
D
x
x/(N/2)·u
u
y
y/(N/2+1)(N/2)·v
v
74"

FIG. 19

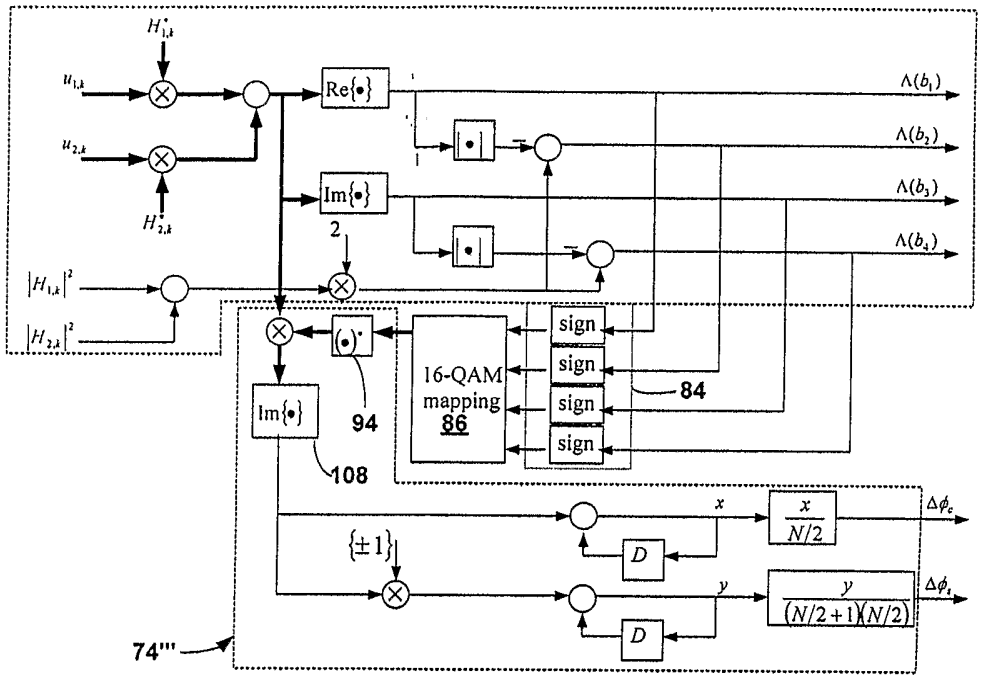


FIG. 20

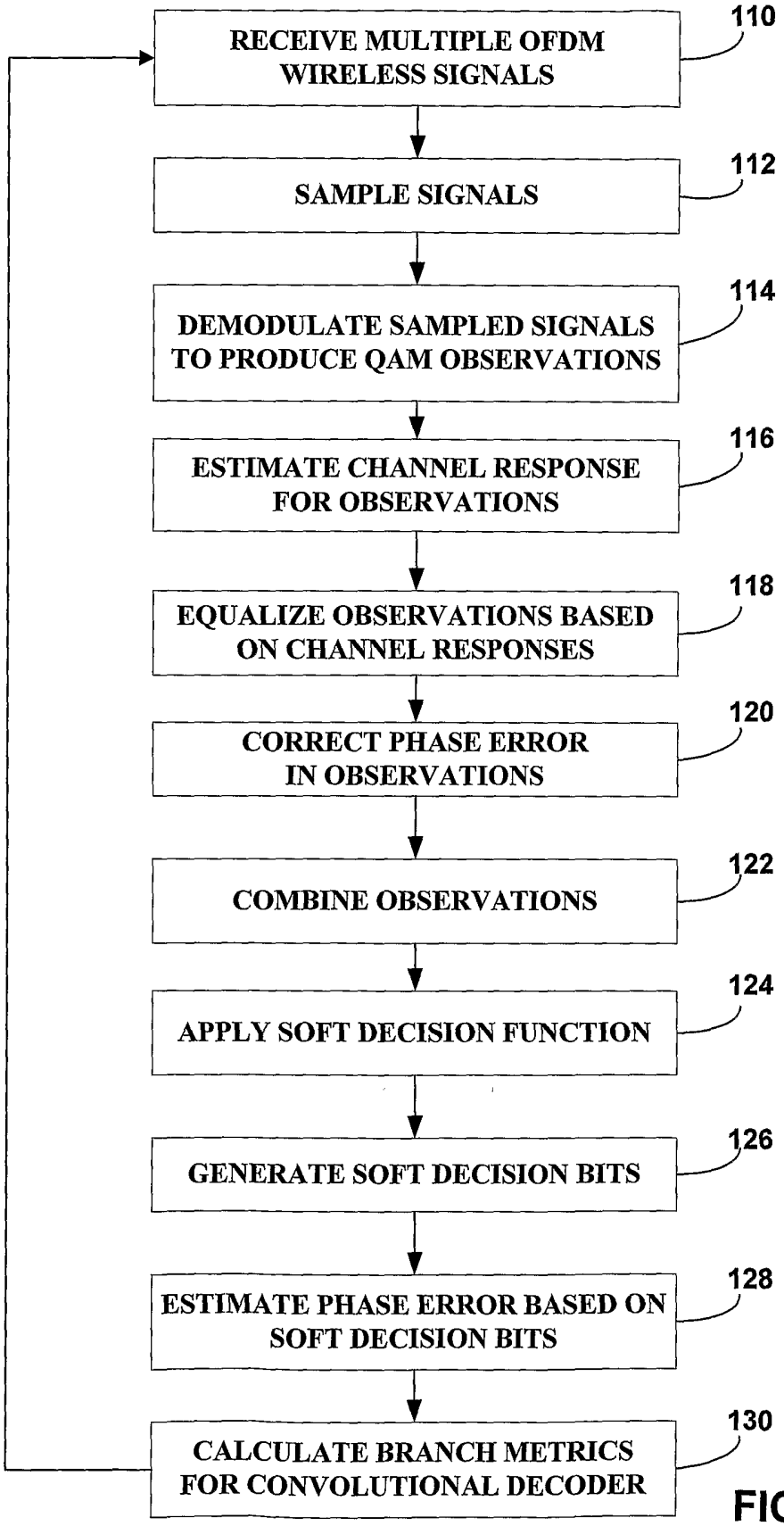

RECEIVE MULTIPLE OFDM WIRELESS SIGNALS
110
SAMPLE SIGNALS
112
DEMODULATE SAMPLED SIGNALS TO PRODUCE QAM OBSERVATIONS
114
ESTIMATE CHANNEL RESPONSE FOR OBSERVATIONS
116
EQUALIZE OBSERVATIONS BASED ON CHANNEL RESPONSES
118
CORRECT PHASE ERROR IN OBSERVATIONS
120
COMBINE OBSERVATIONS
122
APPLY SOFT DECISION FUNCTION
124
GENERATE SOFT DECISION BITS
126
ESTIMATE PHASE ERROR BASED ON SOFT DECISION BITS
128
CALCULATE BRANCH METRICS FOR CONVOLUTIONAL DECODER
130

FIG. 21

INTERNATIONAL SEARCH REPORT

International application No.
PCT/US02/37532

A. CLASSIFICATION OF SUBJECT MATTER

IPC(7) : H04L 27/00, 22, 38.
US CL : 375/347, 261, 267; 455/101, 135, 137.

According to International Patent Classification (IPC) or to both national classification and IPC

B. FIELDS SEARCHED

Minimum documentation searched (classification system followed by classification symbols)
U.S. : 375/347, 261, 267; 455/101, 135, 137.

Documentation searched other than minimum documentation to the extent that such documents are included in the fields searched

Electronic data base consulted during the international search (name of data base and, where practicable, search terms used)
USPAT

C. DOCUMENTS CONSIDERED TO BE RELEVANT

Category *	Citation of document, with indication, where appropriate, of the relevant passages	Relevant to claim No.
A	US 5,732,113 A (SCHMIDL et al) 24 March 1998 (24.03.1998), entire document.	1-25
A	US 6,219,334 B1 (SATO et al) 17 April 2001 (17.04.2001), entire document.	1-25
A	US 6,289,000 B1 (YONGE, III) 11 September 2001 (11.09.2001), entire document.	1-25
A	US 6,320,903 B1 (ISAKSSON et al) 20 November 2001 (20.11.2001), entire document.	1-25

☐ Further documents are listed in the continuation of Box C. ☐ See patent family annex.

* Special categories of cited documents:

"A" document defining the general state of the art which is not considered to be of particular relevance

"E" earlier application or patent published on or after the international filing date

"L" document which may throw doubts on priority claim(s) or which is cited to establish the publication date of another citation or other special reason (as specified)

"O" document referring to an oral disclosure, use, exhibition or other means

"P" document published prior to the international filing date but later than the priority date claimed

"T" later document published after the international filing date or priority date and not in conflict with the application but cited to understand the principle or theory underlying the invention

"X" document of particular relevance; the claimed invention cannot be considered novel or cannot be considered to involve an inventive step when the document is taken alone

"Y" document of particular relevance; the claimed invention cannot be considered to involve an inventive step when the document is combined with one or more other such documents, such combination being obvious to a person skilled in the art

"&" document member of the same patent family

Date of the actual completion of the international search	Date of mailing of the international search report
20 December 2002 (20.12.2002)	04 FEB 2003
Name and mailing address of the ISA/US Commissioner of Patents and Trademarks Box PCT Washington, D.C. 20231 Facsimile No. (703)305-3230	Authorized officer Dung X. Nguyen Telephone No. (703) 305-4892

Form PCT/ISA/210 (second sheet) (July 1998)